

Stony Brook University



OFFICIAL COPY

The official electronic file of this thesis or dissertation is maintained by the University Libraries on behalf of The Graduate School at Stony Brook University.

© All Rights Reserved by Author.

Substrate Chemistry, Mechanics And Morphology Influence Stem Cell Differentiation And Biom mineralization

A Thesis Presented

by

Aneel K. Bherwani

to

The Graduate School

in Partial Fulfillment of the

Requirements

for the Degree of

Master of Science

in

Basic Health Sciences

(Oral Biology and Pathology Track)

Stony Brook University

August 2012

Stony Brook University

The Graduate School

Aneel K Bherwani

We, the thesis committee for the above candidate for the
Master of Science degree, hereby recommend
acceptance of this thesis.

Marcia Simon

**Professor and Graduate Program Director
Department of Oral Biology and Pathology**

Stephen Walker

**Associate Professor
Department of Oral Biology and Pathology**

Miriam Rafailovich

**Professor and Member of Oral Biology and Pathology
Material Science Engineering**

Aaron Segal

**Clinical Assistant Professor and Director Of The Advanced Education
Program in Prosthodontics and Director Predoctoral Prosthodontics
Department of Prosthodontics and Digital Technology**

This thesis is accepted by the Graduate School

Charles Taber

Interim Dean of the Graduate School

Abstract of the Thesis

**Substrate Chemistry, Mechanics And Morphology Influence Stem Cell
Differentiation And Biomineralization**

by

Aneel K Bherwani

Master of Science

in

Basic Health Sciences

(Oral Biology and Pathology Track)

Stony Brook University

2012

Abstract 1: DPSC were obtained from pulp tissues of extracted wisdom teeth under protocols approved by the Stony Brook University Internal Review Board. Primary cells were isolated by enzymatic digestion and used from 3rd-5th passage. For experiments on differentiation, cultures were grown in alpha-MEM supplemented with 10% fetal bovine serum, 0.2 mM L-ascorbic acid 2-phosphate, 2 mM glutamine, 10 mM beta-glycerol phosphate either with or without 10 nM dexamethasone. After 21-days samples were examined using confocal microscopy of cells stained with Alexafluor 488-linked phalloidin and propidium iodide, and by scanning electron microscopy (SEM) and Energy dispersive X-ray Analysis (EDAX). Using SEM, biomineralization was observed on all the substrates in the presence of dexamethasone. In the case of P4VP extensive biomineralization was observed in the absence of dexamethasone, where the deposits were templated along the fibers. Minimal biomineralization was observed on PMMA fibers. EDAX spectra indicated that the deposits on both P4VP and PMMA fibers were comprised primarily of Ca and phosphorous, in a ratio consistent with hydroxyapatite. On PMMA carbonaceous deposits were

observed in the absence of Dexamethasone. OCN and ALP mRNA expression is upregulated on P4VP fibers regardless of induction whereas the same occurs under induction only on PMMA. Proteins conformation on fiber is influenced by morphology and chemistry to affect cell differentiation and biomineralization.

Abstract 2: To test the combined effects of biochemical and biophysical cues on stem cell differentiation, we used the mouse cell line C9 that expresses rhBMP-2 under control of the doxycycline-repressible promoter, Tet-Off. Cultures grown with doxycycline served as control, as did the parent cell line (C3H10T1/2) grown with and without doxycycline. Each cell line was grown on Si wafers coated with spun cast monodisperse polymer films of either polybutadiene (PB) where the substrate mechanical response can be controlled by film thickness, or on partially sulfonated polystyrene (PSS₂₈) where surface charge is controlled by the degree of sulfonation. On PB, the moduli of cells expressing rhBMP-2 varied on day 1 by more than a factor of 2 when the substrate modulus was quadrupled and decreased substantially by day 5. Minimal variation in the moduli was observed for either the C3H10T1/2 cells or the C9 cells in the presence of doxycycline. On PSS₂₈, the modulus of all cells was initially large, but decreased by day 3.

Cell differentiation was monitored by qRT-PCR (OSX, ALP, OCN, BSP, SOX9, COL1A, COLX and ALP) and biomineralization by SEM/EDX. Analyses of 14 day cultures showed that Cells expressing rhBMP-2 appeared osteogenic when cultured on SPS (BSP high, ACAN low) and chondrogenic (ACAN high) when cultured on PB; In the absence of doxycycline, the ECM deposited by the C9 cells was completely biomineralized with calcium phosphate on PSS₂₈, while amorphous carbonaceous deposits were observed for the cells cultured on PB. Because occasional regions with small amounts of calcium phosphate deposition were also observed in C9 cultures grown with doxycycline and in C3H10T1/2 cultures grown with or without doxycycline, on PSS₂₈, some mineralization of the ECM may occur independent of differentiation. These data suggest a model where substrate chemistry may control lineage choice and differentiation

Table of Contents

List of Figures.....	vii
List of Tables.....	viii
List of Abbreviations.....	ix
Acknowledgements.....	xi
Literature Review.....	1
Aim of the Study.....	15
Chapter One.....	16
Introduction.....	16
Material and Methods.....	17
Sample Preparation.....	17
Cell Culture.....	18
Cell plating and Proliferation.....	18
Multipotency and Differentiation Assay.....	18
Staining and laser scanning confocal microscopy (LSCM).....	19
Alazarin Red Staining.....	19
Collagen Staining.....	19
Immunohistochemistry.....	20
Scanning electron microscopy and energy dispersive Xray.....	20
Shear modulation force microscopy (SMFM).....	21
Real Time-Polymerase Chain Reaction (RTPCR).....	21
Results.....	22
Cell growth and morphology.....	22
DPSC are Multipotent.....	23
Cell Adhesion and Mechanics.....	23
Distribution of Collagen and Osteocalcin.....	24
Gene Expression (RTPCR).....	24
Biom mineralization.....	25
Discussion.....	26

Effect on DPSC Differentiation.....	26
Effect on Biomineralization.....	27
Conclusions.....	29
Figures and Tables for Chapter One.....	30
Chapter Two.....	44
Introduction.....	44
Material and Methods.....	45
Sample Preparation.....	45
Cell culture and Induction.....	46
Shear modulation force microscopy (SMFM).....	47
Laser scanning confocal microscopy (LSCM).....	47
Scanning electron microscopy and energy dispersive X-ray.....	47
Real Time-Polymerase Chain Reaction (RTPCR).....	48
Results.....	48
BMP-2 is upregulated in absence of Doxycycline.....	48
Cell Stiffness is influenced by surface mechanics and chemistry.....	49
Gene Expression (RTPCR).....	49
Biomineralization.....	50
Discussion.....	50
Effect of Substrate Stiffness and BMP-2 on lineage specification.....	51
Effect of Substrate Chemistry and BMP-2 on lineage specification.....	52
Conclusions.....	53
Figures and Tables for Chapter Two.....	54
References.....	63

List of Figures

Chapter One	30
Figure 1.1 Cell Proliferation and population doubling time.....	30
Figure 1.2 Cell Morphology between Micro and Nano Fibers.....	31
Figure 1.3 Multipotent Differentiation of DPSC and Stro-1 Expression.....	32
Figure 1.4 Vinculin staining of DPSCs on P4VP& PMMA at 1 week.....	33
Figure 1.5 Cell Mechanics (Shear modulation force microscopy).....	34
Figure 1.6 Pico Sirius Staining on P4VP.....	35
Figure 1.7 Osteocalcin expression (Immunohistochemistry).....	36
Figure 1.8 mRNA expressions of Differentiation Markers.....	37-38
Figure 1.9 Alizarin Red S staining for Biomineralization.....	39
Figures 1.10 SEM-EDAX Analysis (28 Days).....	40-42
Figure 1.11 Protein mediated control of Cell Differentiation and Biomineralization.....	43
Chapter Two	54
Figure 2.1 mRNA expression of h-BMP2 gene normalized to 18SrRNA.....	55
Figure 2.2 Cell Moduli on PB and SPS.....	56
Figure 2.3 Modulus of ECM on PSS ₂₈	57
Figure 2.4 Cell Morphology is influenced by BMP-2.....	58
Figure 2.5 mRNA expression of Osteogenic and Chondrogenic markers.....	59

Figure 2.6 Analysis of biomineralized deposits on PB (SEM-EDAX).....60
Figure 2.7 Analysis of Biomineralized deposits on PSS28 (SEM-EDAX).....61
Figure 2.8 Thickness of Biomineralized Film.....62

List of Tables

Table 2.1 Primer sequences for RTPCR mRNA analysis.....54

List of Abbreviations

ACAN	Aggrecan
ALP	Alkaline Phosphatase
ARS	Alazarin Red S
BMP	Bone morphogenic Protein
BSP	Bone sialoprotein
C3H10T1/2	Mouse embryonic mesenchymal stem cells
C9	C3H10T1/2 transfected with recombinant human BMP-2 under tet-off control
Ca	Calcium
cDNA	Complimentary deoxyribose nucleic acid
Coll	Collagen
DEX	Dexamethasone
DOX	Doxycycline
DPSC	Dental pulp stem cells
DSPP	Dentin Sialophosphoprotein
DMEM	Dulbecco Modified Eagles medium
ECM	Extracellular matrix
EDAX	Energy dispersive X-ray Analysis
EDTA	Ethylenediaminetetraacetic acid
ERK	Extracellular signal-regulated kinases
FBS	Fetal Bovine Serum
GS	Goat Serum
GPa	Gega pascal
HF	Hydroflouric acid
Igf2	Insulin like growth factor-2
IPS	Induced Pluripotent Stem Cells

ITGA5	Integrin alpha 5
LSCM	Staining and laser scanning confocal microscopy
MAPK	Mitogen activated protein kinase
MEM	Minimal Essential Media
MPa	Mega Pascal
MSC	Mesenchymal stem cells
OCN	Osteocalcin
OSX	Osterix
P	Phosphate
P4VP	Poly 4 Vinylpyridine
PMMA	Poly methylmethacrylate
PB	Polybutadiene
PBS	Phosphate Buffered Saline
PS	Polystyrene
PSS ₂₈	Partially sulfonated polystyrene
RGD	Arg-Gly-Asp sequene of amino acid
Rho-A	Ras protein
ROCK	Rho-associated protein kinase
RTPCR	Real Time-Polymerase Chain Reaction
SMFM	Shear modulation force microscopy
TCPS	Tissue culture polystyrene
tet	tetracycline

Acknowledgements:

I would like to thank my advisor **Prof. Marcia Simon** for her utmost support not only academically but she stood out as a mentor in all aspects of life. I feel lucky to have been part of the able team of living skin bank at school of dentistry. Being new to the lab and without any exposure to molecular biology, I was feeling very nervous at start but Dr. Simon went beyond my expectation (and showed lot of patience) to help me think and work like an independent scientist from scratch. I hope to continue contributing to the excellent field of stem cell biology along with my clinical career.

I would also like to thank **Prof. Miriam Rafailovich** for showing me the positive light of everything, even in times when science was unforgiving. None of this work would have been possible without her support and her team at Material Science engineering.

Chung-chueh Chang for his collaborative efforts to piece together this research work. Special thanks for never saying No to anything I needed help with.

Guilia Suarato for doing bulk of the engineering work on this P4VP surface and getting this project from pilot to serious mode.

Qsisi for her help with electrospinning and fabricating PMMA and P4VP substrates.

I would like to thank the family at Living Skin Bank:

Dr. Jay Gao for letting me shadow him and learn the basics of the business and watch with awe one of the best molecular biologist I've seen.

I would like to thank **Dr. Adriana Pinkas-Sarafova** for her invaluable opinions during my research. **Dr. Constantin Chipev** for the energy and life he provided to my morale and experiments when chips were down.

Gabriele Hatch for helping me learn the art of pipetting (I think i can win GOLD at the pipetting Olympics) and cell biology techniques.

Alice Shih for unconditional support during my experiments and keeping me disciplined and up to the task like a mother

Literature Review

The success of any biomaterial and tissue engineered constructs depends on molecular level events that determine subsequent responses of cells and tissue. In tissue culture, stem cell differentiation has traditionally been controlled by the addition of soluble factors to the growth media, receiving more attention until recently where the insoluble component Extracellular matrix (ECM) is found to play an equally important role in cell growth and differentiation. The microenvironment surrounding stem cells includes other cell types as well as numerous chemical, mechanical and topographical cues at the micro- and nanoscale, which are believed to serve as signaling mechanisms to control the cell behavior [1]. Recent advances in bioengineering, material sciences and micro-nano fabrication technologies have directed focus on biomaterials (natural and synthetic) that mimic the ECM in terms of chemistry, morphology and mechanics [2-4]. Improved biomaterials for cell culture not only lead to a better understanding of cell behavior in vivo, but also contribute to the design of scaffolds for tissue replacements.

The challenge is to strike the right balance between substrate mechanics, chemistry, and topography in order to achieve specific and well-controlled cellular response. This will require studying the effect of all variables individually and coupled together to achieve the right combination. Our study will vary substrate factors in combination and highlight the complexity of mesenchymal stem cell response when derived from different sources.

Stem Cells

Differentiated cells from the patient are not sufficient enough to generate artificial tissue construct and therefore there is widespread acceptance for use of stem cells in tissue engineering. Stem cells can be multiplied and then allowed to be differentiated thus providing working command over its use by altering its chemical and/or mechanical environment.

Stem cells are broadly categorized into embryonic, adult and more recently induced pluripotent stem cells (IPS) [5]. Cells from zygote to morula are

considered totipotent and can give rise to the whole organism i.e. they can differentiate into any cell line whereas embryonic stem cells are pluripotent and can differentiate into many cell lines but not all. The adult stem cells however are multipotent and can give rise to few cell lines. IPS cells are generated under experimental conditions by inducing somatic cells to dedifferentiate into pluripotent stem cells. The application of IPS in the domain of tissue engineering is limited as one of the major pitfalls is the outcome of cancerous growth.

Research using embryonic stem cells is growing in interest due to their potential medical applications. Despite this potential, the ethical issue with this cell line has created widespread controversy. This concern has led significant focus on adult mesenchymal stem cells. These are undifferentiated cells that give rise to all cells involved in organization and functioning of various specialized tissues from which they originate. Stem cells can potentially be used to treat cancer, diabetes, bone diseases, tissue loss both congenital and traumatic. As we get older our tissues are less functional with less healing. If the endogenous stem cells residing in each tissue can be stimulated, that might allow enhanced tissue function. Alternatively an engineered tissue grown in-vitro can be grafted for therapeutic purposes.

In adult organism most tissues generally contain a small subpopulation of cells called the adult stem cells with the innate ability to maintain a stem-cell pool by self-replication and generate more committed progenitors. These cells show potential for osteogenic differentiation and Alexander Freidenstein was the first to identify this from cells isolated from the bone marrow [6]. The differentiation potential of these cells was subsequently expanded to include neurogenic, chondrogenic, myogenic and adipogenic-committed cells [7-9] defying the belief held by stem cell biologists that adult stem cells was restricted to the tissues in which they resided. The ability of stem cells to differentiate into specific cell types of non-related tissues is referred to as 'Plasticity'.

Mesenchymal stem cells (MSCs) are pluripotent cells isolated from the bone marrow and various other organs. MSCs of adult and embryonic origin share the unique capacity to self-renew and can differentiate to produce specialized cell

types of osteogenic, adipogenic and chondrogenic lineages. Choosing between the two depends upon the goals of tissue engineering for e.g. replacing large bone defects or forming complex tissue will require cells of embryonic origin due to high proliferation and pluripotency. Up until now the major source of adult MSCs was bone marrow with shortcomings limited to pain, morbidity, and low cell number upon harvest, therefore alternate sources for MSCs have been sought [10]. Recently cells exhibiting these properties have been found in the dental pulp. Dental Pulp Stem Cells (DPSC) ultimately differentiates into odontoblasts, which lay down dentine under physiologic and pathologic conditions

Dental Pulp Stem Cells:

When dental pulp tissue is under physiologic or pathologic stress, damaged odontoblasts degenerate and are replaced by undifferentiated mesenchymal cells that migrate to the injured site from deeper regions of the pulp tissue. These cells differentiate into new odontoblasts in response to BMP, and deposit secondary or tertiary dentine depending upon the severity of insult [11-13]. Reparative dentin is formed towards the root and the remaining pulp becomes smaller. The ability of both young and old teeth to respond to injury by inducing reparative dentin suggests that a small population of competent progenitor pulp stem cells exist within the dental pulp. This group described the identification of dental pulp stem cells (DPSCs) by virtue of their clonogenic abilities, rapid proliferative rates, and capacity to form mineralized tissues both in vitro and in vivo.[14]

Dental pulp stem cells were identified as a significant source of adult pulp stem cells from deciduous as well as permanent teeth by pioneers in the field Gronthos et al [15]. They found this population of cells to follow the basic tenets of stem cell behavior i.e. self-renewal and differentiation potential. Upon transplantation of these cells in-vivo in a mouse a dentine-pulp like complex was formed [14-16]. The cellular characteristics of these DPSC have been compared with those of bone marrow stem cells. Both dental pulp and bone-marrow stem

cell populations express similar putative stem cell surface markers, including CD44, CD106, CD146, 3G5, and Stro-1 [17]. They both expressed matrix proteins associated with mineral tissue formation, such as alkaline-phosphatase, osteocalcin, and osteopontin. Similar expression patterns have been observed for stem cells isolated from periodontal ligament. However, in contrast to bone marrow stem cells, DPSCs have been shown to maintain a 30% higher proliferation rate and a higher growth potential [17]. This higher rate of proliferation has been linked to the increased pulp cell expression of specific cell cycling mediators, namely cyclin-dependant kinase 6 and insulin like-growth factor 1 [18].

When compared to bone marrow stem cells, DPSCs favor formation of dentine at the transplantation site in immunocompromised rats. Gene profile of these cells up regulates Collagen type XVIII alpha1, Insulin like growth factor-2 (Igf2), discordin domain tyrosine kinase 2 and cyclin dependant kinase 6 more than bone marrow stromal stem cells. Furthermore, upon prolong culture there is difference in the regulation of several genes belonging to cell division, cell signal, cell structure and metabolism [18, 19].

Critical to the application of DPSCs in tissue engineering is to quantify the subpopulation of pluripotent/multipotent stem cells in dental pulp. Furthermore these Stro-1⁺ cells also differentiate into adipocyte, myocyte, and chondrocytes when induced by respective cocktail of factors [20, 21]. When cells isolated for Stro-1 were compared with those which were negative for this mesenchymal stem cell marker, only Stro-1 positive cells were capable of differentiating into odontoblast like cells, indicating the importance of these cells in dentine repair processes [22]. A monoclonal antibody that targets a cell surface protein STRO-1 is the most extensively used method in sorting stem cell fraction through Fluorescence-activated cell sorting or Magnetic activated cell sorting from the bone marrow aspirate [23]. Studies show these cells hold multilineage differentiation capacity including osteogenesis [24, 25]. Previous experiments have demonstrated that stem cells isolated from the pulp of human exfoliated

deciduous teeth and expanded in vitro, show approximately 9% positivity for STRO-1, which is considered an early marker of mesenchymal stem cells [15].

Engineered Stem Cells:

Direct gene delivery has focused on transfer of genes in-vivo to influence the cells at site needing engineered tissue. Alternatively cells (differentiated or undifferentiated) have been injected at these sites with hopes of enhancing tissue formation. The goal of engineered stem cells is to combine both the strategies above to produce significant amount of therapeutic proteins. This overcomes the limitations of direct protein implantation i.e. short protein half life, large expensive doses of protein, and potential complications from carriers added with the protein [26]. Overproduction of tissue such as bone is problematic therefore exogenous control of transgene expression is vital and provides control of the therapeutic effect [27, 28]. This is in the form of an inducible expression system such as the C9 cells (mouse embryonic mesenchymal stem cells C3H10T1/2 under tetracycline control) that can be controlled by exogenous introduction of Doxycycline in culture media or in diet, which regulates production of BMP-2 at the site of tissue engineering. This method favors healing of large bone defects which are beyond the body's capacity to generate a larger scale response.

Biomaterials:

Biomaterials are materials intended for use in the human body to replace, augment or interact with the living tissue or function of the body. Biomaterials used as allograft for implantation in bone tissue can be classified according to their chemical composition in ceramics (bioactive glass and hydroxyapatite), metals (titanium and stainless steel), and polymers (polymethylmethacrylate). Metals are commonly used in weight bearing applications, *i.e.* as bone implants. Unfortunately the perfect bone implant material has not yet been developed. All the current biomaterials used in bone tissue tend to loosen over time with the

exception of titanium dental implants that has shown an 82.94% success rate approaching almost 16 years [29]. And as life expectancy increases, the need for revision surgeries also increases. The interactions of implant materials and tissues are complex and they vary depending on both the implant material and target tissue. Although the principles of the processes that take place at the tissue–biomaterial interface are known, the details of these are still largely unknown. A comprehensive understanding of tissue– biomaterial interactions is important for the development of new and for the improvement of old biomaterial applications.

The biological scaffolds used in tissue engineering range from natural to synthetic polymers. While natural materials provide inherent instructive cues for stem cells, they are not without limitations, which include a possible immune response, potential loss of biological activity during processing and insufficient control over mechanical properties. This discussion will therefore focus on the use of synthetic polymers.

Polymers

The commonly used polymeric materials for scaffold fabrication are poly lactic-co-glycolic acid, poly lactic acid, polyhydroxyalkanoates, polycaprolactone and hydrogels such as polyethylene glycol. Among the most employed technologies are phase separation, electrospinning and self-assembly. However, other methods such as melt spinning can be utilized in order to obtain the scaffolds with different properties.

This study focuses attention on non-biodegradable substrates for bone applications. PMMA is a hydrophilic substrate that is FDA approved for in-vivo use showing good biocompatibility with cell growth. It is a common polymer, which is used for micro and nano-imprinting processes. It is an amorphous, thermoplastic polymer with excellent optical transparency and glass transition temperature 105°C.

PMMA has withstood the test of time by replacing lost oral tissues in the form of dental prosthesis; due to its favorable characteristics and low toxicity it has been incorporated by other medical specialties. PMMA has been used as bone cements, contact and intraocular lens, screw fixation in bone, filler for bone cavities and skull defects and vertebrae stabilization in osteoporotic patients. Although numerous new alloplastic materials show promise, the versatility and reliability of PMMA cause it to remain a popular and frequently used material. PMMA does not adhere to bone due to its weak interface with hard tissue and nowadays there are several attempts to improve this biomaterial by the addition of bioactive materials. Despite the weak adhesion of this material with bone there is up regulation of wide array of genes by human osteoblasts, which are associated with ossification, cell adhesion and cell proliferation, similar to the bioactive materials except for adhesion based gene ICAM-1.

P4VP a polymer selected for this study has shown to be biocompatible and support cell proliferation comparable to the industry standard tissue culture Petri dish plastic. P4VP also has similar mechanical properties to polystyrene, and hence, may provide a commercially attractive alternative to tissue culture polystyrene (TCPS). The photo-cleavable property of this polymer has been found to be useful in tissue engineering applications where UVA can be utilized to lift off cultured tissue/cell sheet without significant harm [30]. In addition to novel chemical properties such as amphoteric (acid–base behavior) and amphiphilic (hydrophilic–hydrophobic) characteristics, further modifiable features makes P4VP an exceptional starting material in the design of advanced and smart systems for biomedical applications. P4VP polymer can resist bacterial growth by increasing the surface positive charge (hydrochloric acid and with some alkybromides treatment) [31]. P4VP addresses one of the drawbacks of using implant material i.e. infection response, but it is not clear if how well it can integrate with host tissue. To our knowledge the best application of non-biodegradable implant placement is the Titanium dental implant.

Electrospinning:

The goal of tissue engineering is to recreate the exact environment in-vitro that enables cell differentiation and specialized function. This has been possible with the use of electrospinning. This is an established method for creating polymer and biopolymer fibers [32] ranging from micrometers to nanoscale. The process involves applying a high voltage between the source of solution dispensed in a capillary or syringe and the substrate film. The potential creates a liquid droplet at the tip of one electrode. Additional applied voltage ejects the solution in the droplet toward the counter electrode. One of the advantages of the electrospinning technique is that it is relatively easy to produce large amounts of fibers that closely follow the in-vivo environment without expensive fabrication methods. Many biocompatible polymers have been used to generate nanofibres; these polymers can be either biodegradable or non-biodegradable. Non-biodegradable polymers or polymers that have a longer degradation time than biodegradable polymers offer better structural and mechanical support such as with polymers like Poly-hydroxy butyrate valerate and L-lactic acid and Poly-L-lactic acid [33]. These fibers can be further modified by incorporating pores that improves the scaffolds interaction with cells. These fibers offer a major advantage of enhanced cell adhesion and therefore tissue response [34]. This is a potentially useful property if the ultimate goal of implant is to undergo tissue integration.

Cell Differentiation In Vitro

Biochemical Induction:

Typically, the classical method to control stem cell differentiation is by using biochemical factors. The central theme is that biochemical molecules will bind to the receptors located at the cell membrane resulting in the activation of second messenger such as cyclic adenosine monophosphate, or production of kinases that will in turn initiate a cascade of signaling pathways affecting cellular

responses. Dexamethasone, a synthetic corticosteroid and a potent modulator for osteogenic differentiation of MSCs is widely used in this regard [35]. Dexamethasone supports osteogenic lineage differentiation by binding to specific regulatory proteins within the cell and activating transcription of osteoblast-specific genes. *In vitro*, continuous treatment with dexamethasone transforms the morphology of MSCs from spindle shaped to cuboidal, increases alkaline phosphatase activity, is required for matrix mineralization, and acts at multiple points in the differentiation process to stimulate osteoblastic maturation. If dexamethasone is removed from *in vitro* culture, a population of cells may regress toward a more undifferentiated state or differentiate along alternative pathways, such as the adipogenic lineage; therefore, a continued dexamethasone presence is required to achieve maximal osteogenic differentiation of MSC cultures. It is still unclear as to how osteogenesis is specifically achieved by Dexamethasone, as most of the effects reported are up-regulation of a majority of non-specific factors by Dalby et al. One way in which this is achieved is by upregulation of Integrin alpha 5 (ITGA5) in MSC when it is exposed to dexamethasone i.e. ITGA5 overexpression promotes osteogenesis in-vitro, whereas specific ITGA5 silencing reduced osteoblast marker gene expression and blocked osteogenic differentiation of MSCs [36]. FAK, ERK1/2, and PI3K are necessary for ITGA5-induced osteoblast gene expression, thus identifying major signal transduction pathways that converge to mediate osteoblast differentiation induced by ITGA5 in MSCs. Of notable interest is activation of SMAD by ERK1/2 signaling, further activating protein 1 transcription factors and induces Runx2 phosphorylation, which subsequently induces expression of osteoblast marker genes [37, 38]. In another study dexamethasone in MSCs increases FHL2 protein that interacts with β -catenin and increases β -catenin nuclear translocation. This, in turn, results in activation of TCF/LEF transactivation, increased Runx2, and osteogenic differentiation of MSCs. This describes a novel Wnt/ β -catenin-dependent molecular mechanism, by which dexamethasone and thus FHL2 promotes osteogenic differentiation of MSCs [39].

Bone morphogenetic proteins (BMPs) are potent effectors of MSC differentiation to the osteogenic lineage. However, the levels required for hard tissue regeneration in humans are much higher than expected from animal studies, and patients have shown significant variability in response to BMP treatment [40, 41]. In another study, when compared to natural in-vivo, over six orders of magnitude higher levels of BMP is required to produce the same effect in humans using an artificial matrix [42]. The relative unresponsiveness of MSCs to BMPs and their inability to consistently stimulate bone formation at levels found in the body has enhanced the importance of dexamethasone for osteogenic differentiation of human MSCs.

Biophysical Induction (Cell-Substrate Interaction):

One of the most important aspects of the way biological cells adapt to their environment is their adhesive interaction with the substrate. Numerous aspects of the physiology of cells, including survival, proliferation, differentiation and migration, require the formation of adhesions to the cell substrate, typically an extracellular matrix protein. Fibronectin through its RGD domain favors cell attachment; laminin protein through the presence of various EGF motifs can allow proliferation and its inhibition leading to differentiation and apoptosis. These adhesions also guide diverse processes both by mediating force transmission from the cell to the substrate and by controlling biochemical signaling pathways. Tissue formation involves cell-substrate and cell-cell contact. The cell-substrate interaction is pre-dominant initially followed by the later. Beta actin mRNA expression dominates during an early period of tissue formation because cell adhesion, spreading and migration are closely related to cytoskeletal development that determines cell shape. As cell population rise, mRNA coding for ECM proteins initiate its production [43].

The molecular difference in adherence to substrate can affect the cell outcome in terms of survival, proliferation, differentiation and migration. Traditionally this was achieved through biochemical means. The biophysical aspect of substrate can be fabricated in such a way to achieve desirable cell

behavior. Cell substrate interaction can be classified into three major types: responses due to surface chemistry, responses due to material hardness, and the ones from surface topography. Incorporation of certain moiety on the surface was shown to be favorable for cell to attach. For example, the presence of certain peptide sequences, such as a RGD sequence, on surfaces increases cell attachment [44]. In addition, the degree of hydrophilicity was shown to affect cell attachment to the surface.

The effect of stiffness on stem cell differentiation is best exemplified by Engler et al [45] in which polyacrylamide gels of varying stiffness and constant collagen I concentration were used to examine MSC behavior. This sensing of matrix elasticity is mediated by Non-muscle Myosin II, which in association with actin is involved in generating force through focal adhesion contacts. When pre-osteoblasts are exposed to soft and stiff RGD-functionalized PEG gels, they express higher levels of activated MAPK and osteocalcin on the stiffer surface. Activation of MAPK (through phosphorylation) has been associated with focal adhesions and further downstream activation of Runx2, which regulates osteocalcin and ALP expression. RhoA is another molecule involved in the generation of intracellular tension, and is influenced by matrix mechanics in both differentiated and undifferentiated cells. Changes in RhoA expression in MSCs seeded on soft and stiff polyacrylamide gels resulted in different Ca^{2+} oscillations [46]. MSC Ca^{2+} oscillations are controlled by ROCK, a downstream effector molecule of RhoA, and therefore can be modulated by the mechanics of the substrate.

The second factor important in surface modification is incorporation of nanotopography and micro patterning. The ultimate goal is to mimic the architecture of extracellular environment around the cell. ECM environment is rich in proteins conferring nanoscale topography that affects cell-matrix interaction such as collagen which is approximately 1.5 nm wide and 300 nm long [47]. Furthermore these molecules form fibrils which are tens of micrometer in length and 260-410 nanometers in diameter [48]. By using a bio-inert material i.e. TiO_2 and vertically aligning them in nano-tubule form the authors were able to

dictate cell behavior using defined diameters between 15 and 100 nm and show that adhesion, spreading, growth, and differentiation of mesenchymal stem cells are critically dependent on the tube diameter [49]. Spacing less than 30 nm with a maximum at 15 nm provided an effective length scale for accelerated Integrin clustering/focal contact formation and strongly enhances cellular activities compared to smooth TiO₂ surfaces. Cell adhesion and spreading were severely impaired on nanotube layers with a tube diameter larger than 50 nm, resulting in dramatically reduced cellular activity and a high extent of programmed cell death. Recent developments in advanced micro- and nanofabrication techniques have enabled the fabrication of substrates that mimic native topography on 2-D substrates. These topographical changes vary from nano-fibres, nano-roughness, nano-grating, nano-posts and nano-pits [4].

The enhanced differentiation of MSCs in the absence of osteogenic supplement has also been explored using nanopit arrays. Osteoprogenitor cells and MSCs were cultured long-term on PMMA nanopit arrays of varying order by Dalby et al [50]. The symmetry and order of the nanopits was found to significantly affect the expression of osteopontin and osteocalcin, two bone-specific ECM proteins, in both cell types. While MSCs cultured on completely ordered or completely random nanopits did not lead to expression of these two proteins, MSCs cultured on slightly irregular substrates did exhibit significant amounts of these proteins of interest. Increased bone nodule formation was also evident in MSCs cultured on these substrates relative to substrates with either completely ordered or completely random features. Human MSCs were also cultured on three specific substrates: 1) nanopits, 2) planar substrates in the presence of dexamethasone (DEX), a soluble factor that can induce bone formation (positive control), and 3) planar substrates without DEX (negative control). Human MSCs cultured on nanopits expressed a similar level of many osteoblast-specific genes when compared to MSCs cultured on flat substrates in the presence of DEX. Furthermore, some genes were specifically upregulated in MSCs cultured on nanopits compared to MSCs cultured with DEX alone. The results from these two studies demonstrate the potential of nanotopography to

direct cell fate. Furthermore, the complementary findings of MSCs cultured on nanogratings and ordered-disordered nanopits suggest the potential for selective, controllable differentiation based solely on the geometry of the nanotopographic substrate. One key function that could directly connect nanotopographic signaling to cell responses is spatially biased focal adhesion formation through Rho activation, which could have dramatic downstream effects on cell migration and signaling.

Local mechanical control of stem cell microenvironments can also be accomplished by patterning colonies of cells [51]. In this study MSC aggregates were grown on patterned cell adhesive surfaces. They observed patterns of differentiation that corresponded with local strains experienced by cells. In rounded aggregates, a radial pattern of differentiation was observed where cells in the center were committed to an adipogenic lineage and cells in the periphery were driven to an osteogenic lineage. Additionally, from the results of further complex patterns it was concluded that the magnitudes of forces at the convex edge were nearly three times those at the concave edge (66.3 vs. 23.6 nanonewtons per post) and mirrored the pattern of osteogenic versus adipogenic differentiation. Furthermore they tested whether the high tension generated at convex edges is responsible for increased osteogenesis at those edges and treated MSCs in such patterns with the nonmuscle myosin II inhibitor blebbistatin. Inhibiting myosin-generated tension abrogated osteogenesis almost completely, while preserving adipogenesis.

Cells sense their environment through integrin, and ligand binding to integrin leads to activation of focal adhesion kinase (FAK). A recent study found that on reducing FAK mRNA levels by more than 40%, there is a decrease in ECM-mediated phosphorylation of FAK Y397 and ERK1/2. Serine phosphorylation of Runx2/Cbfa-1 is significantly reduced after 8 days in FAK negative MSCs [52]. They also concluded that FAK inhibition blocked osterix transcriptional activity and the osteogenic differentiation of hMSC, as assessed by lowered expression of osteogenic genes (RT-PCR), decreased alkaline phosphatase activity, greatly

reduced calcium deposition. These results suggest that FAK signaling plays a vital role in regulating ECM-induced osteogenic differentiation of hMSC.

Biom mineralization:

The mineral phases of enamel, dentin, and bone are apatites differing in crystallinity, with the enamel mineral showing considerably higher crystallinity than either dentin or bone. The focus of this discussion is the distinction between dentinogenesis and osteogenesis. Although bone and dentin are similar in their matrix protein composition, their organ structures are totally different. One of the most striking characteristics is that BMSCs and DPSCs can generate a bone/marrow organ structure and a dentin/pulp complex, respectively. During dentinogenesis, calcium and phosphate ions are transferred from the vascular bed proximally to, and to a certain extent between, the odontoblasts into the organic matrix of dentin in order to be incorporated into dentin mineral. This mineral *phase* comprises, in principle, crystals of hydroxyapatite $\text{Ca}_{10}(\text{OH})_6(\text{PO}_4)_4$. This mineral has a non-perfect crystallinity, is somewhat calcium-deficient, and contains other ions such as carbonate and Fluoride [53]. The mineral crystals in dentin are associated with the collagenous matrix, in that they are largely arranged with their c-axes parallel with the collagen fibers.

The difference of biom mineralization between bone and dentine formation is the absence of remodeling of dentine. The cells primarily involved in formation of dentine are odontoblasts, which are terminally differentiated cells that synthesize several collagenous and non-collagenous proteins. The major phosphoproteins of the non-collagenous group are now known as the SIBLING (small integrin binding ligand, N-linked glycoprotein) family [54]. The SIBLING family consists of dentin matrix protein 1, dentin sialophosphoprotein (DSPP), osteopontin, matrix extracellular phosphoglycoprotein, and bone sialoprotein (BSP). Each of these proteins plays an important role in either promoting tissue mineralization or inhibiting the process. Out of these Dentin Matrix protein-1, dentin sialoprotein, and dentin phosphophorin. These proteins are synthesized by the odontoblasts

during the start of the mineralization process and play a regulatory role during the formation of the dentin matrix.

Aim Of Study:

The biomaterials have been modified in chemistry, morphology and mechanics to study behavior of adult mesenchymal stem cells (human) and embryonic mesenchymal stem cell (mouse) on these surfaces. This study has been divided into two parts. In our first study we asked whether surface topography and/or chemistry affect stem cell differentiation and biomineralization. We also determined as part of our second study whether substrates could determine lineage choice.

Chapter One

Can Substrate Morphology Influence Stem Cell Differentiation And Biomineralization

Introduction:

Most papers focus on the correct soluble mediator required for differentiating mesenchymal stem cells into osteoblasts, chondrocytes, adipocytes and hepatocytes by the use of supplemented mediums [1]. These mediators in the form of growth factors, cytokines, hormones and drugs are used in media to often determine stem cell plasticity and may be limited to in-vitro use due to lack of physiologic correlation in-vivo. The synthetic glucocorticoid dexamethasone induces osteoblastic differentiation and is often included in the osteogenic medium [2]. However, glucocorticoids are also known to induce apoptosis of osteoblasts and osteocytes, which is consistent with clinical glucocorticoid-induced osteoporosis[3]. Hence, there is a move to finding alternatives to chemical inducers of stem cell differentiation and achieve this through substrate/scaffold that mimics the natural ECM environment (spontaneous differentiation). Fabricating the substrate in this manner provides predictability of events as a result of specific cellular response when in contact with implants. Engler was able to show this by varying substrate mechanics with stiffness that correlate with neural, muscular and bone tissue without presence of soluble induction factors [4]. A recent study by Dalby indicates that a non-chemical technique could be nearly as good with use of slightly disordered nanopits on PMMA [5]. However, no study has shown this effect through use of biomimetic fibers at both micro and nano scale. PMMA is a FDA approved material for *in vivo* use in a wide number of applications, ranging from bone fillers to dentistry. However, a deeper investigation of its bioactivity needs to be performed. In this study, attention has been focused on the ability of this polymer to promote biomineralization.

P₄VP is a photo-cleavable polymer, easy to process, that can be readily made

antibacterial. It is also biocompatible and can support cell adhesion and growth without any additional protein coating. Previous results showed that P₄VP supports proliferation rates of neonatal human dermal fibroblasts and human keratinocytes comparable to the standard tissue culture plates [6]. This study will explore the role of varying fiber morphology and chemistry using a biocompatible polymer P₄VP poly-4-vinylpyridine. This will be compared to PMMA (polymethylmethacrylate), which is an excellent control substrate to study the effect of morphology with least influence from the chemistry and physical properties of the material both in static and dynamic terms.

Material And Methods:

Sample Preparation:

P₄VP flat film was prepared by spin casting 3mg/ml in DMF on silicon wafers/glass coverslips at 2500 rpm for 30 seconds and annealed at 150C in vacuum overnight. Micro fibers were electrospun on these 200nm films with the solvent ratio of EtOH:DMF (10:2, w/w), polymer concentration of 25% by wt, and voltage of 18 kV, feed rate 0.1ml/h with a target tip distance of 10cm and 5min deposition rate. Nano fibers were electrospun on 200nm films with the solvent ratio of EtOH:DMF (50:50, w/w), polymer concentration of 15% by wt, and voltage of 15 kV, feed rate 0.1ml/h with a target tip distance of 10cm and 10min deposition rate. Flat film thickness was 10nm, Microfiber diameter ~ 6.8 um and Nanofiber was 128 nm.

For PMMA (M_w=120,000 M_w/M_n>2.65) films, 100 nm thick, were spun cast onto Si wafers or glass cover slips. Solutions of 20wt% PMMA were prepared in Chloroform and electrospun on top of the films. A motorized roller was used to control the fiber spacing and create the patterned surfaces. Samples were then annealed in an oil trapped vacuum oven (10⁻³ Torr) at 120C (T~T_g) for 8 hrs (to remove solvent and sterilize the fibers) [since ethanol cracks PMMA]

The micro fibers had an average diameter of 9.06 um, whilst the Nanofibers had an average diameter of 649 nm.

Cell Culture

Dental pulp stem cells (DPSCs) strain AX3 were isolated from the third molar teeth (IRB #20076778) as previously described and were grown in α -MEM media (Invitrogen) supplemented with 10% fetal bovine serum, 200 μ M L-ascorbic acid 2-phosphate (Sigma Aldrich), 2 mM L-glutamine, 100 units/ml penicillin/ 100 μ g/ml streptomycin, and 10mM β -glycerophosphate (Sigma Aldrich). As control, osteogenic induction of the DPSC was achieved by addition of 10^{-8} M Dex (Sigma-Aldrich). DPSCs from passages 4 through 5 passages were used for all the experimental procedures and incubated at 37°C in a humidified atmosphere with 5% CO₂ and 95% air.

Dermal fibroblasts at 4th passage were used as control cells for SEM-EDAX analysis to rule out biomineralization in the absence of differentiation. The cells were grown in DMEM with 10% FBS and 100 units/ml penicillin/ 100 μ g/ml streptomycin.

Cell plating and proliferation

DPSCs were harvested using Trypsin-EDTA by incubating at 37°C and 5% CO₂ for 5 minutes. Cells were counted and then plated on TCPS, PMMA and P4VP films at a density of 2,000 cells/cm². For the study of cell proliferation, the cell number was determined on day 1, 3,4,5,6 and 7 using Hemacytometer (Hausser Scientific).

Multipotency and Differentiation Assays

For analysis of differentiation, DPSCs were grown on tissue culture plastic for 21 days and evaluated for Osteogenic, chondrogenic and adipogenic differentiation using Alazarin Red-S (ARS), Alcian Blue and Oil Red O staining, respectively. Stemness was further evaluated by measuring the expression of *stro1* at 4 days post-plating. The media used for differentiation were as follows:

Osteogenic Differentiation: α -MEM media (Invitrogen) supplemented with 10% fetal bovine serum, 200 μ M L-ascorbic acid 2-phosphate, 2 mM L-glutamine, 100

units/ml penicillin/ 100 µg/ml streptomycin, 10mM β-glycerophosphate and 10⁻⁸ M Dex (Sigma-Aldrich).

Chondrogenic Differentiation: High glucose DMEM with 10% FBS, 50 mg/ml L-ascorbic acid (Sigma), 6.25 µg/ml Insulin (Sigma) and 10 ng/mL TGF-β[7].

Adipogenic Differentiation: High glucose DMEM 10% FBS, 5 mg/mL insulin (Sigma), 50 mol/L indomethacin (Sigma), 1mmol/L dexamethasone (Sigma) and 0.5 mmol/L isobutyl-1-methylxanthine (Sigma)[7].

Staining and laser scanning confocal microscopy (LSCM)

Alazarin red Staining:

To determine mineralization related to calcium content of DPSC cultured on PMMA-P4VP flat film, microfiber and nanofiber scaffolds at 7, 14, and 21 days of culture. This was based on ARS staining dye, which binds selectively calcium salts. Samples were washed three times with PBS and fixed with 10% Buffered Formalin for 15 minutes, washed two times carefully with distilled H₂O and then stained with 1% ARS for 5 min at room temperature. After several washes with distilled H₂O to remove excess dye, scaffolds were examined under the optical microscope.

Collagen Staining: This method is based on the selective binding property of the syrius-red dye to the (Gly-X-Y) tripeptide end sequence of mammalian collagen [8]. After removing culture media at day 7 all samples on P4VP were washed with PBS, followed by fixation with Bouin's fluid for 1 h. After fixation, the fixation fluid was removed and the culture dishes were washed by immersion in running tap water for 15 min. The culture dishes were air dried and stained by 1% Sirius Red (in aqueous solution of Picric acid) dye reagent for 1 h under mild shaking on a shaker. Thereafter, the solution was removed, and the cultures were washed with 0.01 N HCl to remove unbound dye. Pictures were taken immediately under optical microscope. Rat-tail collagen type 1 was used as positive control whereas samples cultured with media only for 7 days and uncultured samples as negative controls.

Immunohistochemistry

For IHC, DPSCs were washed with PBS, fixed with 3.7% formaldehyde solution for 15 minutes, and permeabilized with 0.4% Triton X-100 in PBS. To visualize actin the cells were incubated with 1:200 dilution of Alexa Fluor 488 Phalloidin solution (Invitrogen, Carlsbad, CA). The nuclei were visualized by propidium iodide (Sigma Chemical Co., St. Louis, CA) by adding 5ug/ml for 5 minutes. Samples were imaged using a Leica TCS SP2 LSCM (Leica micro-system Inc., Bannockburn, IL). For detection of osteocalcin, cells were incubated for 30 minutes at RT with a blocking solution comprising 10% goat serum (GS) in PBS, washed twice with PBS and then incubated for one hour with a 1:100 dilution of the rabbit anti-osteocalcin antibody (Santa Cruz) in 1%GS/PBS solution. Samples were washed twice with PBS (5min) and incubated for 30 minutes at 37C with a 1:200 dilution of Texas red conjugated goat anti rabbit secondary antibody (Santa Cruz) in 1%GS/PBS. Nuclei were visualized with DAPI-mounting media (Vectashield, Vector Laboratories Inc, Burlingame CA) and samples transferred to glass slides to be imaged with inverted microscope. For detection of Stro-1, cells were incubated with 1:100 dilutions of mouse-antihuman Stro-1 antibody (Santa Cruz). Antibody followed by incubation with FITC goat anti-mouse IgM antibody (Santa Cruz) at a 1:200 dilution, which was visualized using a Nikon 880 microscope.

For Vinculin Stain Monoclonal Anti-Vinculin antibody produced in mouse, clone hVIN-1, ascites fluid (Sigma-Aldrich) was used with Oregon Green® 488 goat anti-mouse IgG (H+L) at 2 mg/mL as secondary.

Scanning electron microscopy and energy dispersive X-ray (SEM/EDX)

Surface morphologies of PMMA and P4VP films were characterized using scanning electron microscopy (SEM, LEO1550, LEO, German) at 20 kV acceleration voltage and 10 mm working distance. Samples were prepared by gently washing with DI water to remove soluble salts from media and air-drying for 1 day. Samples were sputter-coated with gold for 15s and loaded on

aluminum stubs for SEM imaging. The elemental compositions of deposits on PMMA and P4VP films were determined by using Energy dispersive X-ray spectroscopy in conjunction with SEM. Samples from PMMA and P4VP were also treated to 1% Osmium tetra oxide, 1% tannic acid in PBS (after fixing with 10% buffered formalin for 15 minutes) and increasing concentrations of ethanol from 20% to 96% for imaging DPSC's on SEM.

Shear modulation force microscopy (SMFM)

The moduli of DPSCs cultured on PMMA and P4VP films (Flat, Microfiber and Nanofiber) were measured by atomic force microscopy (AFM, Dimension 3000; Digital Instruments, Santa Barbara, CA) on shear modulation force microscopy (SMFM) mode. The experimental setup of the SMFM method is described in earlier articles. Briefly, the AFM tip, applied to indent the surface, was laterally modulated and the mechanical response was fed into a lock-in amplifier and recorded. During the measurement, a normal indenting force of 25nN was exerted by the cantilever to maintain tip-surface contact, while a sinusoidal drive signal was applied to the piezo controlling the cantilever to induce a small oscillatory motion. The lateral deflection (response) amplitude of the cantilever was measured against the drive amplitude, both in mV, the response amplitude, therefore, being proportional to drive amplitude.

Real Time-Polymerase Chain Reaction (RT-PCR)

On day 7,14,21,28 and 35 after cell seeding the cells were trypsinized and resuspended as cell pellet. The cell pellet was lysed and stored at -80° C for a maximum period of one month. The total RNA was extracted from DPSC and on PMMA and P4VP using Qiagen RNeasy kit (RNeasy kit, Qiagen, Valencia, CA). 1µg of total RNA was reverse-transcribed with 200 units/reaction Superscript II Reverse Transcriptase (Invitrogen) into cDNA using 200ng/reaction of random primers (Invitrogen). The obtained cDNA was used as a template in PCR. Specific markers for osteocalcin (OC), bone sialoprotein (BSP), alkaline phosphatase (ALP) and Dentin Sialophosphoprotein (DSPP) monitored

osteogenesis versus odontogenesis. The sequences of the specific primer for 18SrRNA are forward GTAACCCGTTGAACCCATT, reverse CCATCCAATCGGTAGTAGCG; Alkaline Phosphatase ALP are forward GTACTGGCGAGACCAAGCGCAA, reverse ACCCCACACAGGTAGGCGGT; OCN forward ATGAGAGCCCTCACACTCCTCG, reverse GTCAGCCAACTCGTCACAGTCC; DSPP forward GCATTTGGGCAGTAGCATGG, reverse CTGACACATTTGATCTTGCTAGGAG. 18SrRNA were used as a housekeeping gene to normalize mRNA expression. Due to its abundant expression 18SrRNA cDNA was diluted 100 times before use in the PCR. Real-time PCR was performed using SYBR Green PCR kit (Qiagen, Valencia, CA) and controlled in a DNA engine MJ Opticon 2 thermal Cycler with continuous fluorescence detection (MJ Research Incorporation, Union, NJ). DNA amplifications were performed under the following conditions: 95 °C (15min), 94°C (30 s), 55°C (30 s), and 72 ° C (30 s) for 40 cycles, A melting curve program was performed immediately after the above cycling program in order to generate a first derivative dissociation curve for each sample and dilution series by using the instrument's software. Each sample was assessed in triplicate.

Results

Cell growth and morphology

Cell growth analysis showed that PMMA P4VP did not show significant effects on cell growth with respect to its control (TCPS). The cell doubling time (DT) was 26 hours for DPSCs seeded on P4VP. This is comparable to TCPS with a DT of 27 hours. DT on PMMA i.e. 30 hours was longer than P4VP and controls perhaps due to initial lag phase where ECM is being laid down. (Figure 1.1) Stem cell morphology was evaluated at Day 5, 14 and 21. Morphology was not conclusive. The cells appear more flattened on the flat surface (not shown). There is tendency for cells to align with fibers regardless of dexamethasone and less so

on nanofibers. Cells appear more elongated on PMMA compared to P4VP. Figure 1.2)

DPSC are Multipotent

DPSC differentiation was evidenced by the formation of mineralized nodules (odonto-osteogenic), lipid vacuoles in the cytoplasm (adipogenic) and mucopolysaccharide matrix (chondrogenic) after 21 days of treatment with the respective induction media (Fig.1.3 A-G). The positive staining was not observed in the respective negative controls (cultivated in regular medium). The control media involved absence of DEX, TGF β -insulin and IBMX-Indomethacin-DEX in the osteogenic, chondrogenic and adipogenic samples respectively.

Multipotent mesenchymal stem cells express STRO-1 surface marker. We checked for Stro-1 expression on 5th passage DPSC that are typically used for all experiments through immunohistochemistry and mRNA expression on TCPS. Stro-1 expression was observed by IHC in about 36% of cells population. This expression was confirmed by mRNA where it is down regulated under induction where progressively more cells differentiate and lose their stemness. In the absence of DEX expression of Stro-1 was upregulated. By definition Multipotent stem cells should be able to adhere to plastic and undergo division, undergo differentiation into multiple lineages and express stem cell marker i.e. Stro-1. Results from our experiment support the above definition except that almost half the population expressed STRO-1 since we did not sort for pure stem cell fraction. (Figure 1.3 H-J)

Cell Adhesion and Mechanics

The distribution and arrangement of the focal adhesion points (FAP) is related to how cells are sensing the substrates. Vinculin density is more apparent ON P4VP samples compared to PMMA. There is an increase in FAC on fibers compared to flat surfaces. This might be due to increase in surface area, as fibers are Electrospun on the flat surfaces. The FAP are more aligned along the fibers than in between. This factor is responsible for creating tension across FAP

that results in induction towards osteogenic lineage. (Figure 1.4 A-L)

Using Shear modulation force microscopy, DPSC show complex mechanical behavior on P₄VP with higher cell moduli on fiber samples without induction and all inductive samples except for microfiber group. However all control PMMA surfaces show increase in cell modulus that is dependent on induction with Dexamethasone. (Figure 1.5 A-B)

Distribution of Collagen and Osteocalcin

Figure 1.6 (A-F) illustrates histological staining of DPSC on P4VP showing increased Sirius red collagen content in the fiber samples and flat substrate induced by DEX compared with controls. Collagen I deposition is essential prior to the event of mineralization when bone/dentine is being formed. There is an increase in PSR staining on all induced surfaces (more so on fibers than flat). There is also an increase of collagen distribution on non-induced fiber samples (micro and nano fibers) independent of DEX compared to flat surface. The staining of cells and fibers correlate with the subsequent biomineralization observed on P4VP samples. Osteocalcin immunostaining was positive for P4VP samples on fibers independent of DEX and induced samples on PMMA. (Figure 1.7 A-B) The cells on microfiber sample on P4VP show expression of OCN. compared to the adjacent flat area.

Gene Expression (RT-PCR):

To evaluate the effects of the polymer substrates on stem cell differentiation, we performed RT-PCR analyses for genes associated with hard tissue formation in DPSC cultures grown on PMMA and P4VP at different times of their differentiation (1,14,21,28 and35). RT-PCR analyses (Figure 1.8 A-C) revealed differences for OCN expression, both on the P4VP and PMMA surfaces. ALP expression (A) was higher on Day 28 for microfiber and nanofiber samples (flat, microber and nanofiber). OCN expression (B) was higher for microfiber and nanofiber samples without induction and all induced samples (flat, microfiber and

nanofiber) on P4VP and PMMA at day 28 and 35. There is was a general increased expression of DSPP (C) on P4VP surface compared to PMMA suggesting a more odontogenic response on P4VP, particularly the microfiber and nanofiber samples independent of dexamethasone.

Biom mineralization:

Biom mineralization was assessed using ARS dye which stains calcium salts (Figure 1.9) By day 21, P4VP fibers showed enhanced ARS staining on fibers independent of dexamethasone. Since Calcium staining occurs over time and more efficiently on fibers, substrate morphology is likely the driving force in the biom mineralization process. However PMMA showed no significant increase in the intensity of calcium staining until 21 day. ARS staining at 28 day for PMMA showed enhanced staining dependant on dexamethasone irrespective of morphology. Compared to P4VP the staining of Calcium is predominantly between the fibers. This indicates the biom mineralization on PMMA is based on DPSC differentiation and is not substrate driven.

SEM-EDAX was used to analyze mineralized deposits for the presence of Ca, P and Carbon. SEM was performed on day 28 samples using DPSC, Control dermal fibroblasts and with no cell in the presence of media. All surfaces induced with DEX showed biom mineralized deposits (Figure 1.10 A-H). These deposits comprised of Ca-P as observed on the EDAX spectrum. The deposits on P4VP were templated on and off the fibers, whereas deposits on PMMA did not show any predilection for fibers. Cells can be visualized on the induced deposits (Figure 1.10 G and H). DPSC is adequately anchored on the PMMA fiber that was not pre-coated for cell adhesion, indicating its biocompatibility for cell growth. In non-induced samples (figure 1.10 I-P) only the P4VP samples with fibers showed significant deposits templated along fibers in both Micro and Nano fibers that comprised Ca-P. The few deposits seen on PMMA without induction were carbonaceous in nature. Presence of deposits that are templated on P4VP fibers highlights the importance of morphology and chemistry at play with use of this polymer. This can also be appreciated when visualized with cells on SEM

(Figure O-P). Differentiation and Cell independent biomineralization was also observed along the Micro fiber samples on P4VP (regardless of presence of DEX) (Figure Q-T) and Nanofibers (Data not shown). This may indicate that proteins from media change their conformation when adsorbed on the P4VP fibers that initiate biomineralization independent of cells and differentiation.

Discussion:

The key feature a cell responds to when interacting with biomaterials is the adsorbed proteins on its surface upon immediate contact with blood or serum. The conformation of these adsorbed proteins is likely to influence the cell adhesion, migration and possibly proliferation on the substrate [9]. Cell biomaterial interaction is complex, since it is mediated through adsorbed proteins from the environment and those produced by the cells. We hypothesized that by changing chemistry and morphology (ultimately influencing adsorbed protein conformations) we can influence stem cell differentiation and biomineralization in the absence of a soluble mediator. (Figure 1.11) To test this model we chose DPSC and cultured them on two selected polymers i.e. PMMA and P4VP that vary in chemistry and topography. Three different morphologies were tested; flat films obtained by spin casting and micrometric and nanometric fibers obtained by electrospinning. Dental pulp stem cells were chosen for this study since they have been found to respond marginally better in bone tissue production when seeded with non-biodegradable implant for osseointegration. In a recent study DPSC resulted in mean bone-implant contact values of $66.7\% \pm 3.6\%$ compared to $62.5\% \pm 3.1\%$ for bone marrow stem cells and $39.4\% \pm 2.4\%$ for Periodontal cells [10].

Effect on DPSC Differentiation:

DPSC were cultured on flat films, microfibers and Nanofibers made of P4VP and PMMA to determine the effect of morphology on stem cell differentiation. Osteocalcin, Alkaline Phosphatase and Dentin Sialophosphoprotein expression was evaluated on DPSC till 35 days. DPSC on P4VP showed no response to

DEX as ALP and OCN were up regulated in response to substrate morphology by day 35 except for flat films where late response was observed under induction. In contrast all differentiation on PMMA was mediated by DEX independent of substrate morphology. The expression levels of DSPP were higher on P4VP indicating odontogenic inclination especially on fiber samples where the levels were up regulated till day 35 compared to flat P4VP and PMMA controls. Stem cell response to differences in surface morphology largely relates to the adsorbed proteins and the integrins that are expressed on the cell membrane [9]. This expression of integrins in terms of quality and quantity can vary by changes in morphology of the substrate [11]. Most studies identify Focal adhesion contacts as significant in terms of differentiation of stem cells. We have looked at vinculin (part of FAC) immunostaining on all surfaces with DPSC that was not conclusive. Generally there is higher expression of FAC on P4VP than PMMA substrates that is indicative of the role of substrate in dictating stem cell response.

Effect on Biomineralization:

Biomineralization was observed on PMMA substrates on induction with DEX. There was no effect of morphology on stem cell response. The scarce deposits visible in the absence of DEX were carbonaceous which may indicate a cellular stress response. However on P4VP an effect of morphology was clearly noted. SEM-EDAX identified Ca-P deposits on all surfaces with fibers independent of DEX induction. ARS staining for calcium on these substrates by day 21 confirmed these results. Biomineralization on Flat surface was under control of induction. The effect of morphology is clearly at play here. This correlates with increase in cell modulus at day 7 on PMMA, where induction resulted in increase cell stiffness. These findings are consistent with studies showing biomineralization is preceded by increased cell modulus at an earlier time point. On P4VP this relationship was not consistent and appears more complex as all surfaces undergoing biomineralization were preceded by increased cell modulus

except for microfiber sample under induction where modulus remained unchanged. Perhaps further study is needed to confirm or rule out this difference. Biomineralized deposits on P4VP were mostly templated along the fibers both at the micrometer and nanometer scale. Some deposits were also present in micro and nano fibers on P4VP in the presence of control cells (dermal fibroblasts) and those fibers that were cultured in the absence of cells. Presence of deposits on control surfaces with fibers on P4VP indicates the importance of morphology and chemistry. It is our understanding that the curvature modifies the structure of adsorbed proteins from media and cell, exposing cryptic domains that are involved in biomineralization independent of dexamethasone. This change in conformation of adsorbed protein originating from serum and cell secretion enables binding of Ca and P to initiate the biomineralization process. Additionally, this phenomenon may also aid in differentiation of stem cells as osteogenic markers are up regulated in the presence on fibers. The stable conformation of the secreted ECM proteins is resulting from the balance between an enthalpy term, related to the chemistry of the substrate, and an entropy term, depending upon the surface topography. In addition this conformation also results in stem cell differentiation towards the osteogenic/odontogenic pathway independent of dexamethasone.

Variations in surface chemistry may be mediated through different composition and bioactivity of adsorbed proteins, its involvement in directing a particular response to morphology is less clear. There is some evidence that proteins adsorb differentially with variations in surface roughness [12]. When comparing proteins adsorbed from serum on smooth versus fibrous PLA poly (L- lactic acid), there was difference in quantity and quality suggesting a mechanism separate from increase in surface area. In their study, nano-fibrous scaffold adsorbed greater amounts of fibronectin and vitronectin, which enhanced osteoblast attachment [11]. To our advantage this was corroborated in our study where keeping the same approximate surface area across polymers, P4VP showed spontaneous cell biomineralization templated along fibers at both micrometer and nanometer level compared to PMMA controls. Further studies are required to test

the in-vivo safety of these fibers when using with implants to enhance integration with host bone tissue.

Conclusions:

The role of surface chemistry was explored by contrasting the influence of substrate induction on dental pulp stem cells. Dental pulp stem cells were plated on flat and fibrillar substrates composed of two glassy polymers with comparable mechanical properties ($T_g \sim 100^\circ\text{C}$, $M \sim 10\text{GPa}$).

On P₄VP biomineralization does not correlate with up regulation of osteogenic markers. Large amount of biomineralization occurs on fibers independent of dexamethasone indicating surface curvature is responsible for initiating biomineralization that does not seem to be correlating with cell differentiation. Interaction between cell and materials is interesting but complex and therefore prior to internal use materials must be investigated thoroughly.

1. Dexamethasone is required to induce DPSC on PMMA, regardless of substrate modulus or topography.
2. Surface curvature is sufficient to generate deposition of biomineralized deposits on P₄VP substrates independent of dexamethasone, or up regulation of osteogenic markers
3. Since cell dependant and independent biomineralization was observed on P₄VP we propose that ECM proteins are adsorbed differently due to different interactions with the two polymers and in addition the curvature.
4. On P₄VP curvature modifies the structure of adsorbed ECM proteins exposing cryptic domains that are involved in biomineralization.

Figures:

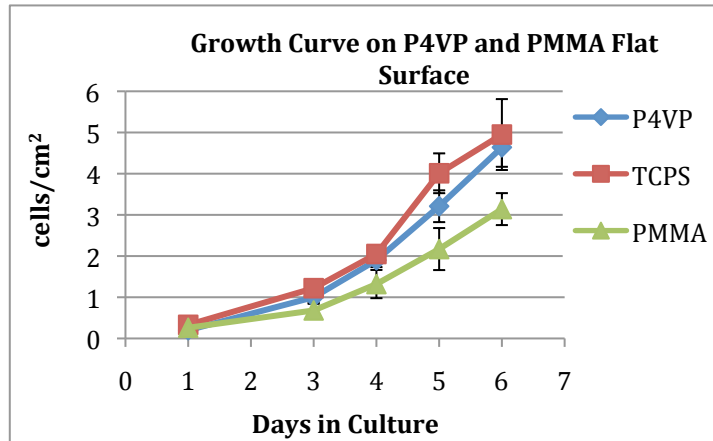


Figure 1.1 Cell Proliferation and population doubling time

The DPSC growth on PMMA, P4VP and TCPS is shown from day 1, 3,4,5 and 6. 2000 cells/cm² were plated on day 0. There is an initial lag phase on PMMA followed by increase in cell growth resulting in an overall higher doubling time of 30 hours compared to 25 hours on P4VP and 26 hours on control TCPS. 1=10,000 cells

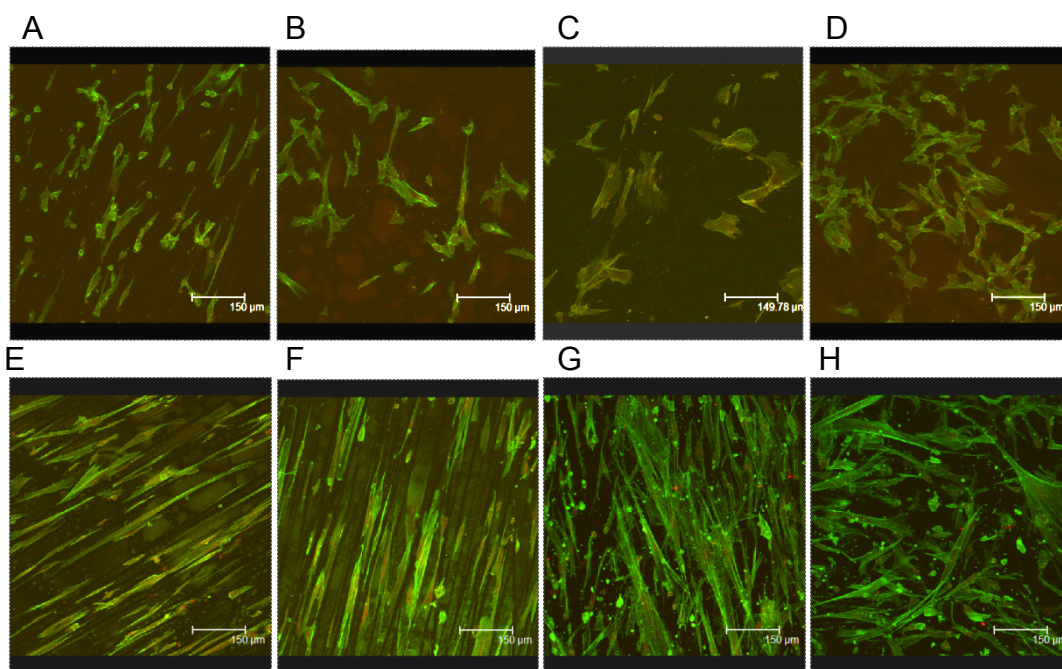


Figure 1.2 Cell Morphology between Micro and Nano Fibers

A-D (day 7) shows P4VP samples, E-H (day 7) shows PMMA samples. Cells on fibers appear elongated as seen in ABEF. More elongation is observed on PMMA micro fibers (EF) compared to the same on P4VP (AB).

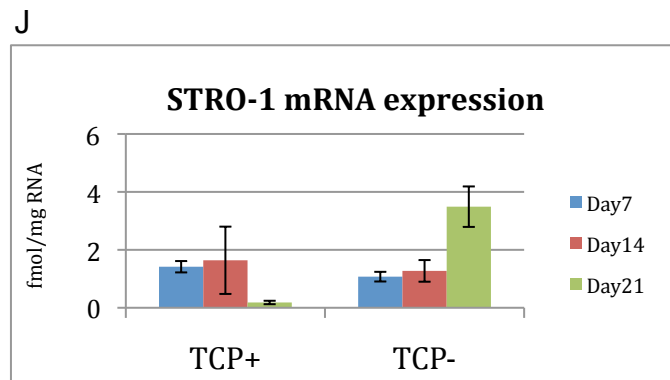
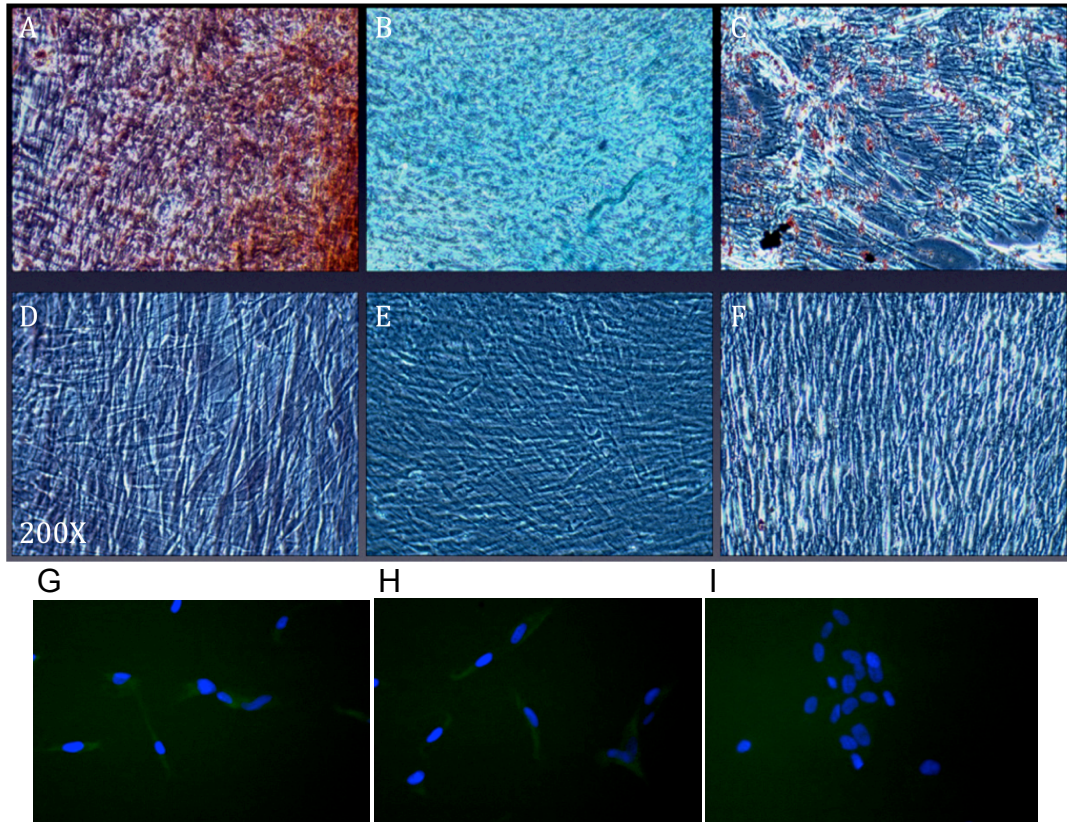


Figure 1.3 Multipotent Differentiation of DPSC and Stro-1 Expression
 Differentiation assays on TCPS: A & D odonto-osteogenic; B & E chondrogenic C & F adipogenic. A shows mineralization stained with Alizarin red; D negative control after Alizarin red staining. B exhibits chondrogenic differentiation of DPSC after containing regions of matrix mucopolysaccharide stained with Alcian blue; E shows negative controls after Alcian blue staining. C shows Adipogenic differentiation of DPSC displaying lipid vacuoles in the cytoplasm stained with Oil red O; E shows negative controls after Oil red-O staining. All images obtained at 200 times magnification. IHC shows expression on Stro-1, G-H for stem cells. Image I shows secondary only control. All images are at 400 times magnification. This expression was checked at mRNA level on TCPS where this marker is down regulated under induction and upregulated in the absence of DEX.

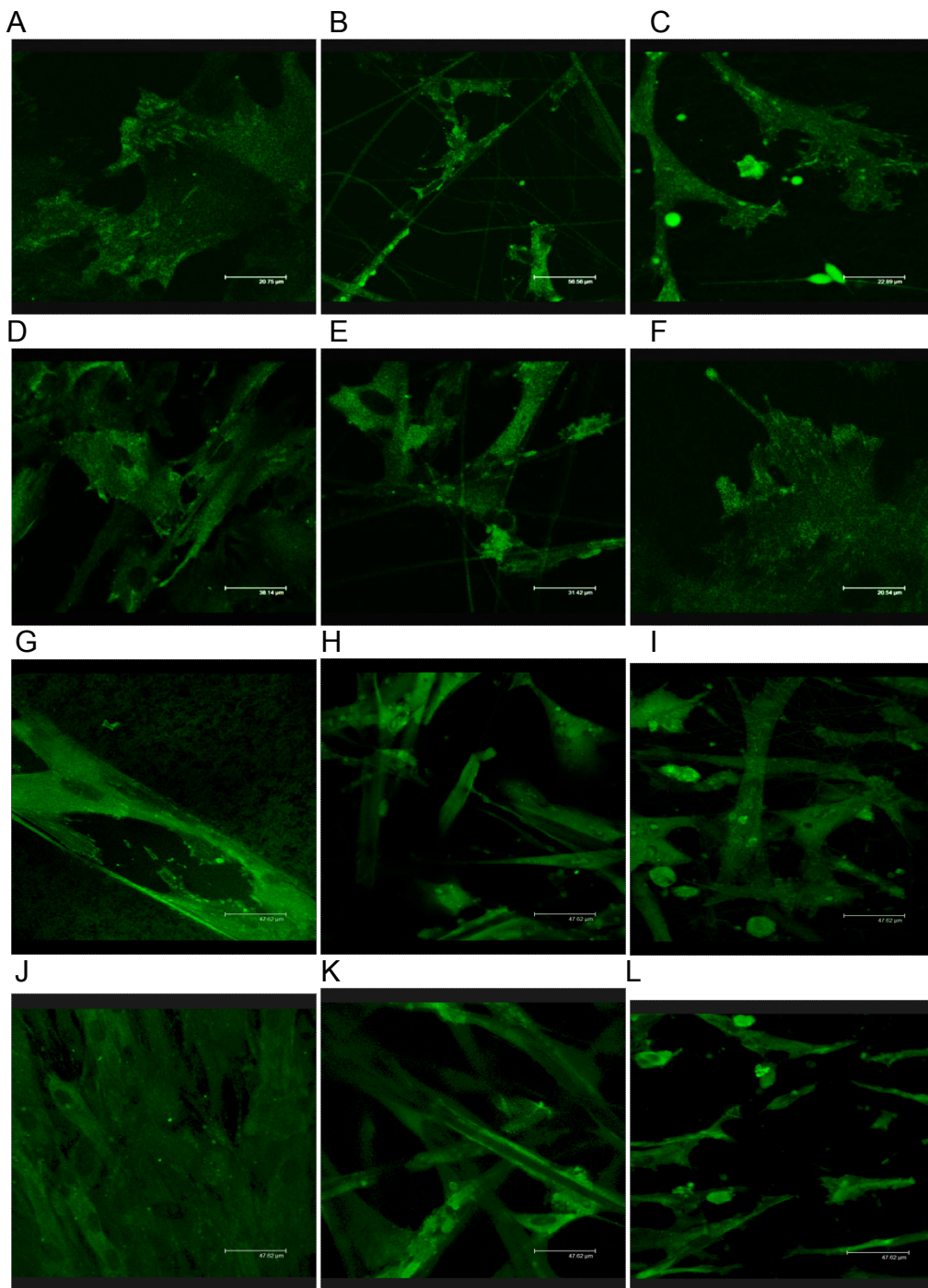
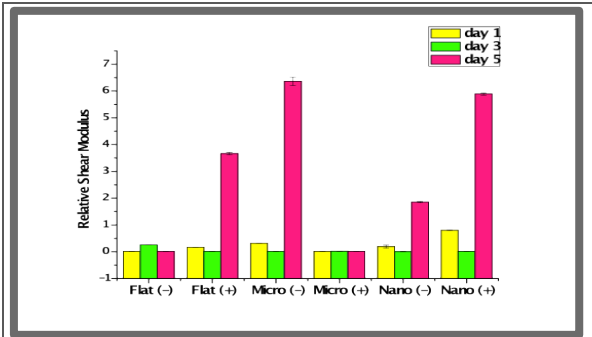


Figure 1.4 Vinculin staining of DPSCs on P4VP& PMMA at 1 week
 A-C are P4VP samples induced with DEX; D-F shows non-induced P4VP samples. A and D are Flat films, B and E are Microfiber samples whereas C and F are nanofiber samples. G-I are PMMA samples induced with DEX; J-L are PMMA non-induced surfaces G and J are Flat films, H and K are Microfiber samples whereas I and L are nanofiber samples. Overall more FAC are seen P4VP compared to PMMA.

A



B

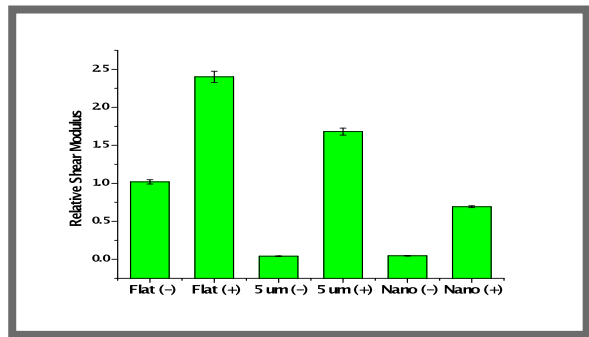


Figure 1.5 Cell Mechanics (Shear modulation force microscopy)

A= Relative Cell moduli on P4VP (day 1-5)

B= Relative Cell moduli on control PMMA (day 5)

There is increase in Modulus on all surfaces under induction except for Microfibers on P4VP. There is an increase in cell modulus by day 5 on microfiber samples by a factor of 3 compared to nanofiber under non-induction on P4VP substrates.

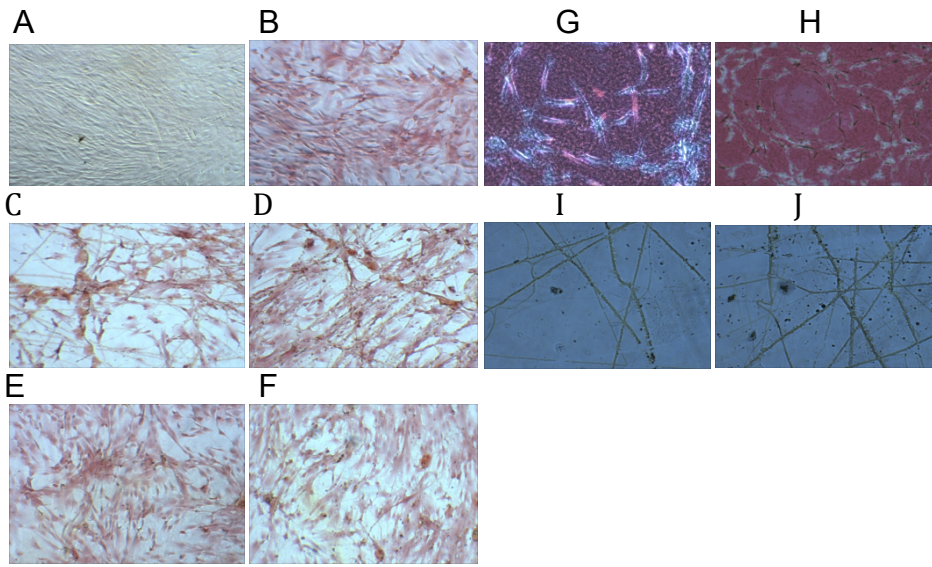


Figure 1.6 Picosirius Staining on P4VP

Pico-Sirius red stain stains for Collagen. ACE shows non-induced samples whereas BDE shows induced (with DEX) samples. AB is the Flat film, CD is microfiber and EF is the nanofiber substrate. GH shows rat-tail collagen type I controls which were plated with DPSC for 21 days in G and without cells on H. IJ shows no cell controls on P4VP microfibers. I is dry un-incubated sample whilst J was incubated with media only for 7 days.

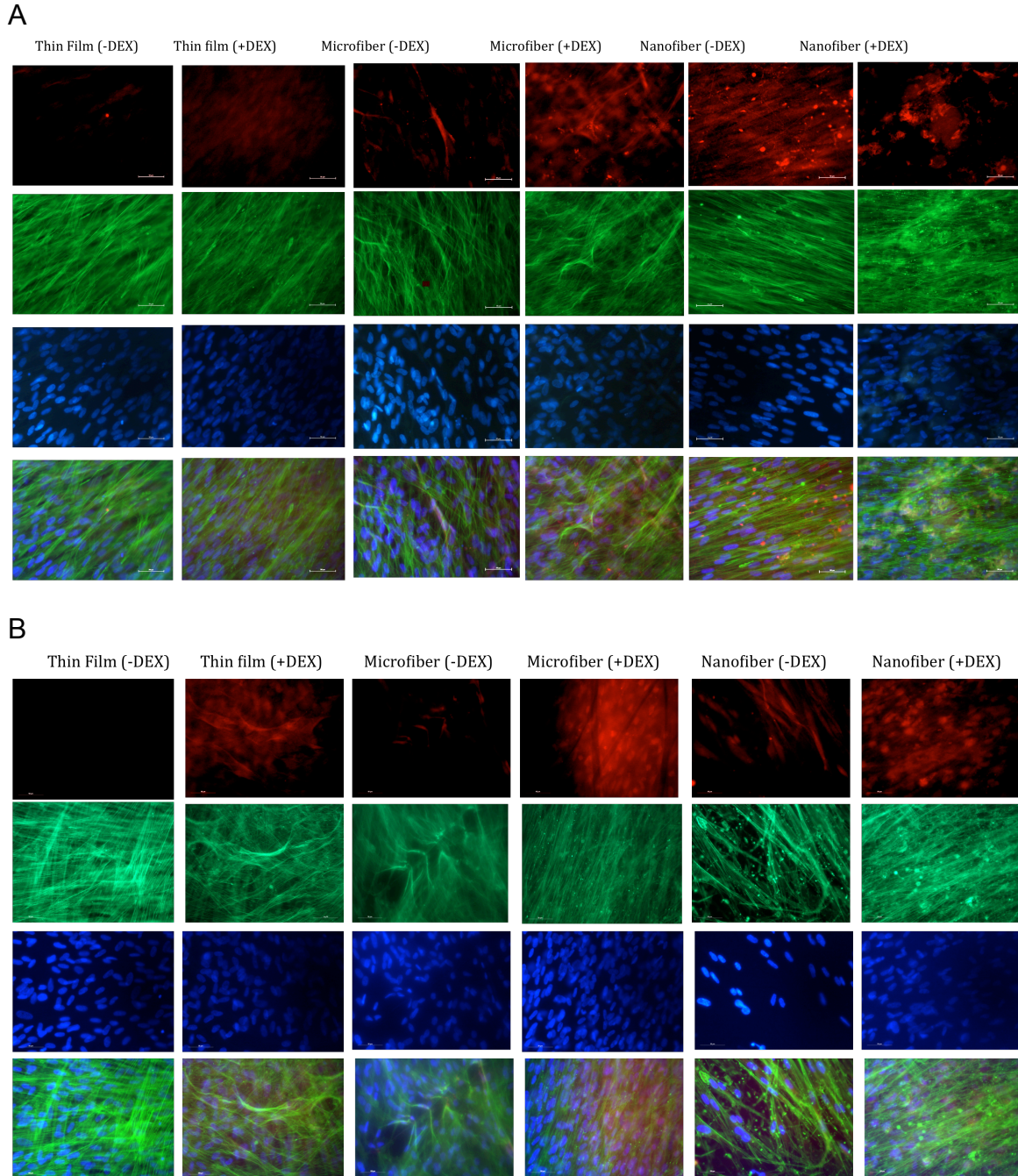
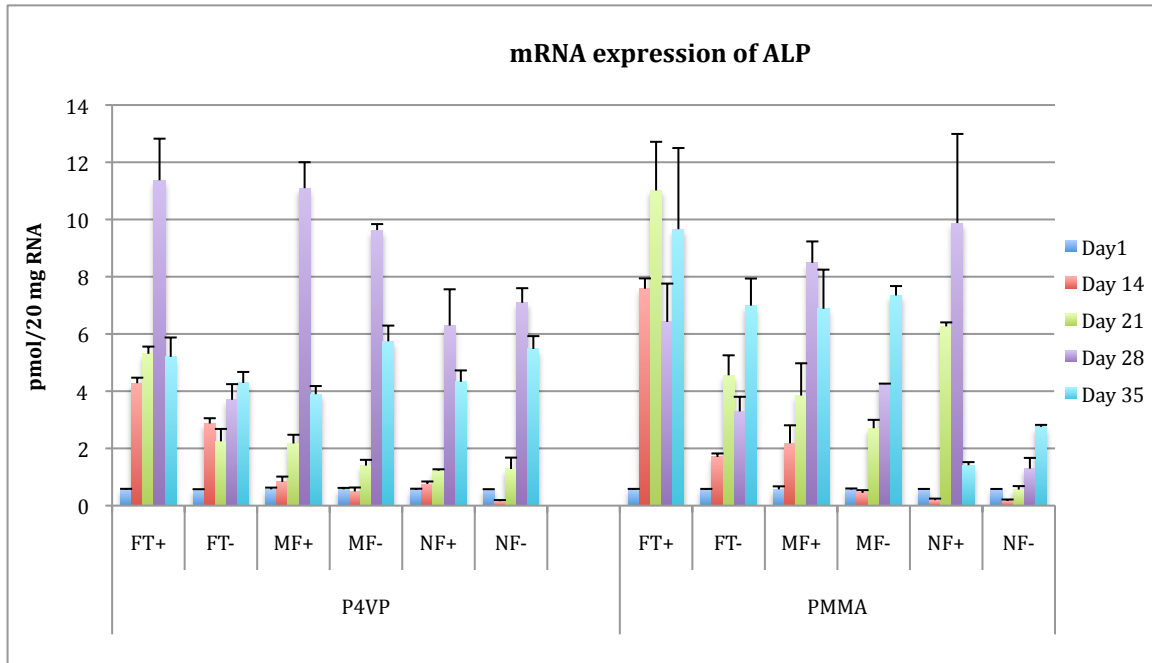
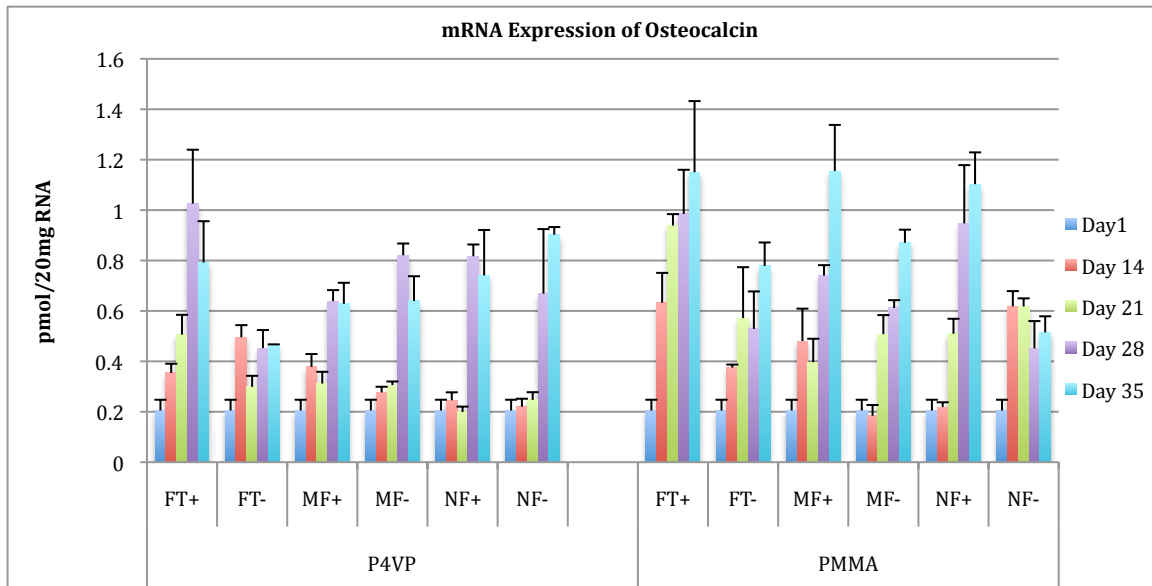
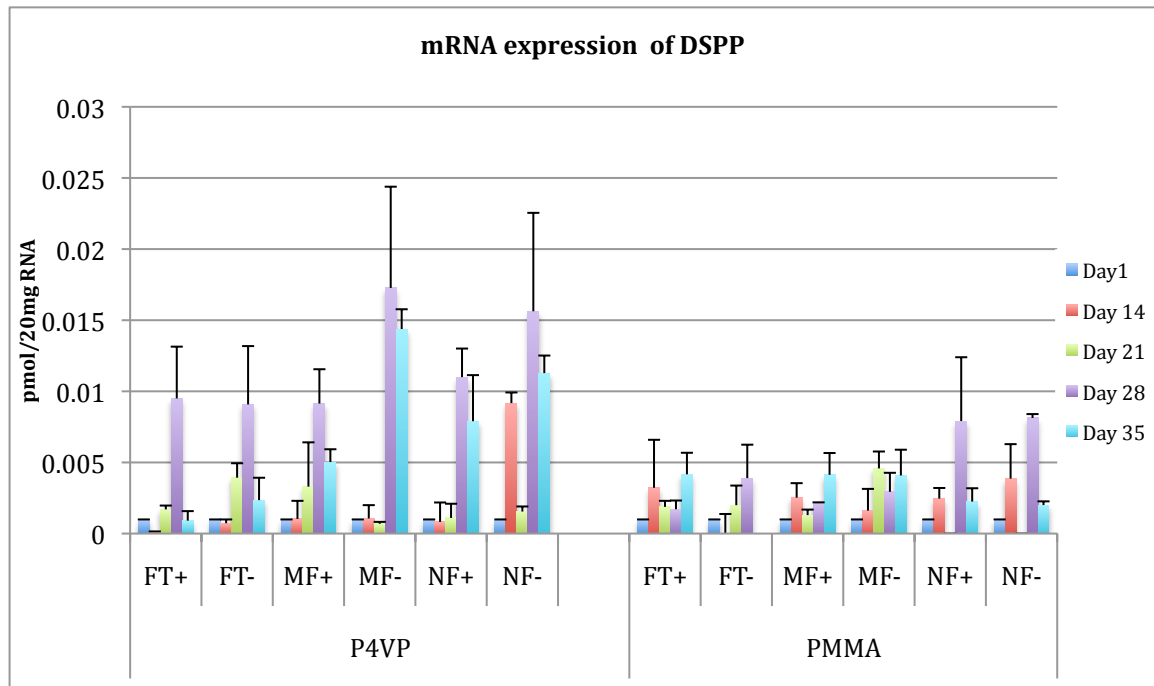


Figure 1.7 Osteocalcin expression (Immunohistochemistry)

A shows Osteocalcin expression on P4VP. B shows Osteocalcin expression on PMMA. Red indicates osteocalcin expression (Texas red). Green indicates actin staining with Alexaflour 455. Nuclei are counterstained with DAPI and shown in blue. The bottom row on A and B shows merged images on all surfaces from P4VP and PMMA (Flat, Microfiber and Nanofiber samples)

A**B**

C**Figure 1.8 mRNA expressions of Differentiation Markers**

A shows regulation of ALP and B shows regulation of OCN. C shows regulation of DSPP by both surfaces and fiber samples. Alkaline Phosphatase on P4VP (A) and PMMA show upregulation by 28, which is significant relative to flat non-induced surfaces. Expression of Osteocalcin (B) is higher on all surfaces at day 28 and 35 on P4VP compared to flat non-induced. The same is seen for PMMA at day 28 and 35. There is generally higher expression of DSPP on P4VP compared to control PMMA indicating differentiation on P4VP being more odontogenic as opposed to osteogenic on this surface.

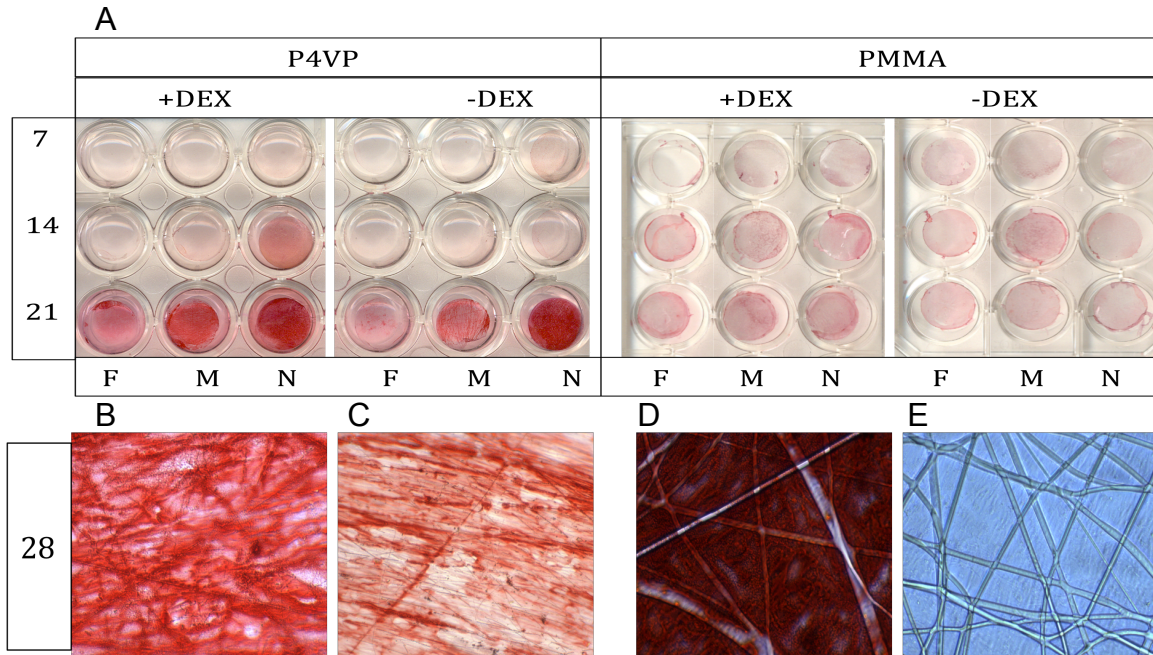
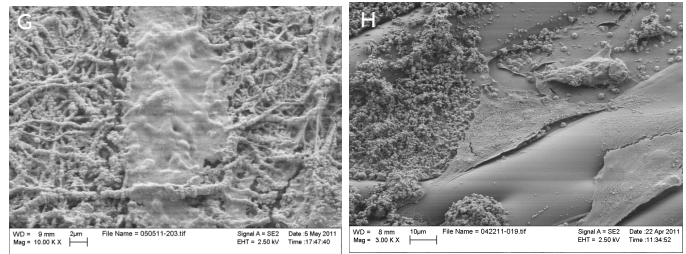
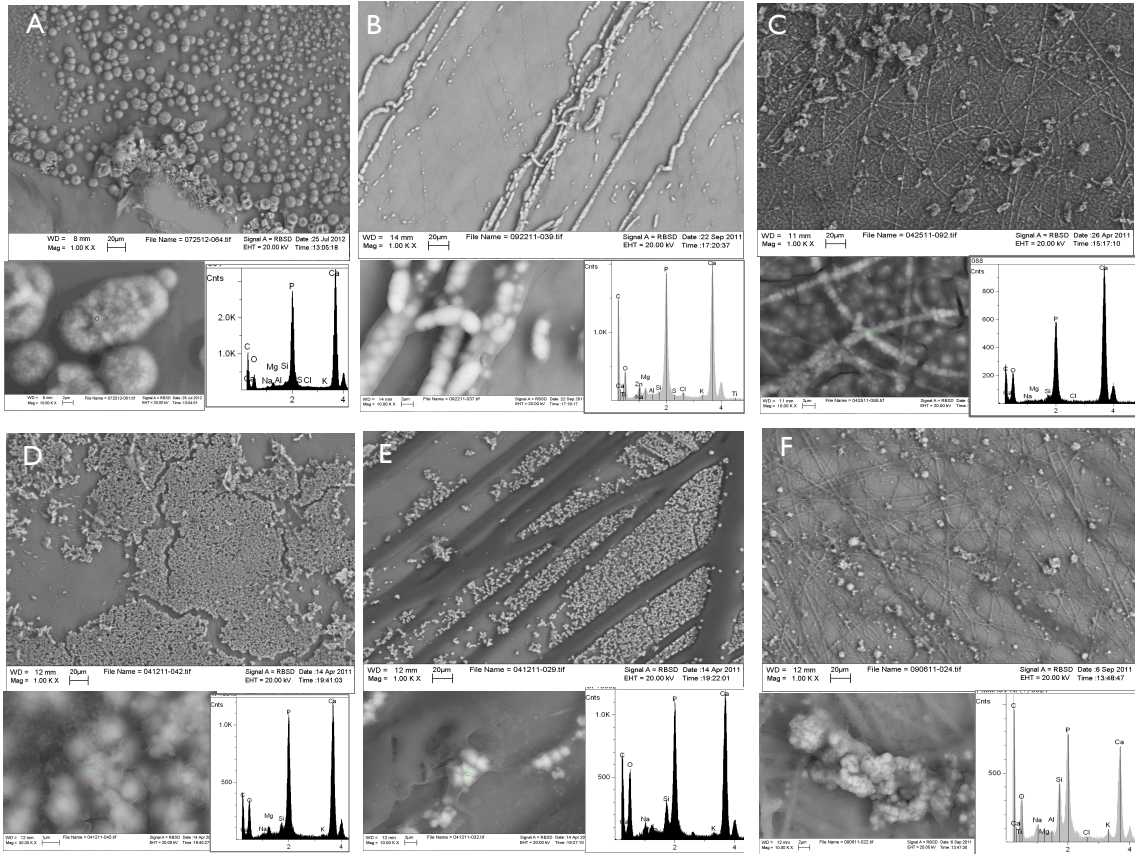
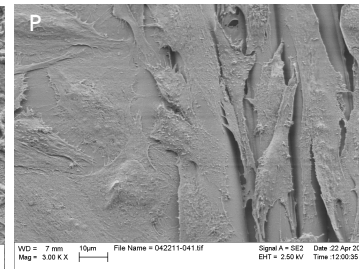
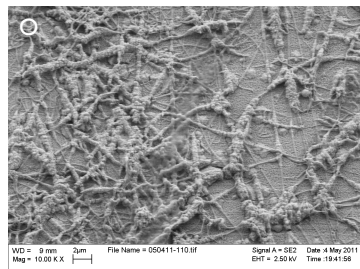
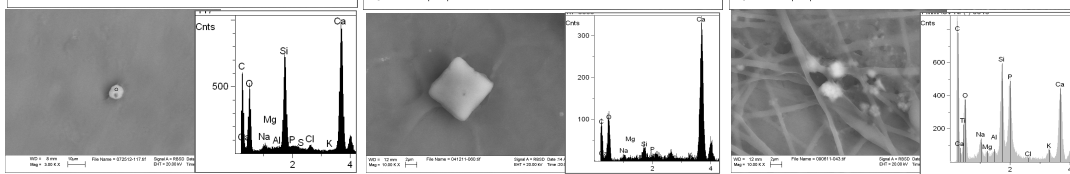
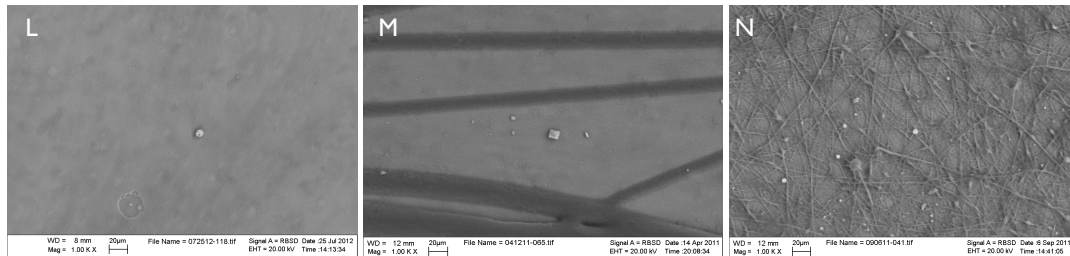
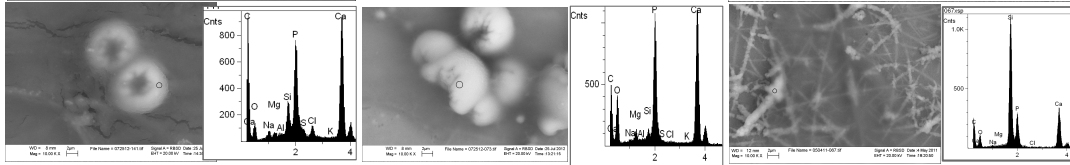
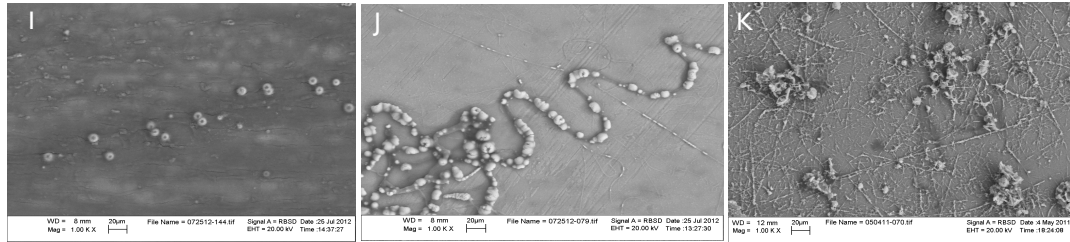


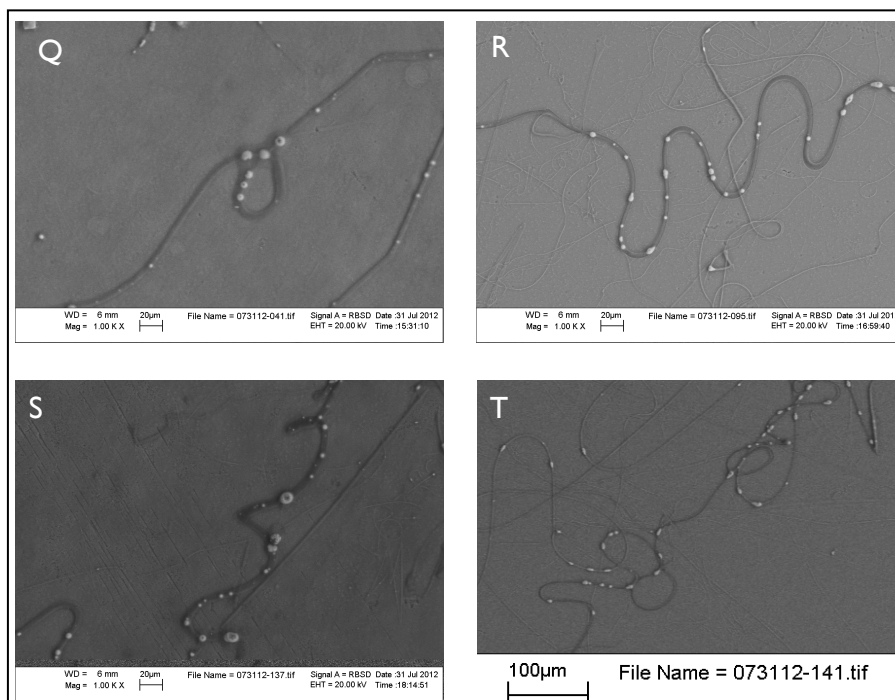
Figure 1.9 Alizarin Red S staining for Biomineralization

A shows ARS staining on P4VP and PMMA samples (F=Flat film, M=Microfiber and N=Nanofibers on glass cover slips) in a 24 well plate incubated with DPSC for 7,14 and 21 days. P4VP shows ARS staining by day 21 independent of DEX. PMMA shows no significant change in intensity till day 21.

B and C show 28 day ARS histological staining on Microfiber samples for P4VP independent of induction. D and E show the same for PMMA but DEX dependant. B and D are induced with Dex whereas C and E are non-induced samples.







Figures 1.10 SEM-EDAX Analysis (28 Days)

DPSC and Dermal Fibroblasts along with no cell controls were incubated on P4VP and PMMA samples (Flat, Microfiber and nano-fiber) for 4 weeks under induction media and non-induction media.

A-H shows Induced samples on P4VP and PMMA with DPSC. I-P shows Non-induced samples with DPSC. QS shows micro fibers on P4VP plated with Dermal Fibroblasts and RT shows no-cell controls on P4VP microfiber sample.

A shows induction on flat surface P4VP with biomineralized deposits with Ca-P peaks on spectrum. B and C show the same on Micro fibers and Nano fibers respectively. D shows induction on flat surface PMMA with biomineralized deposits that correlate Ca-P peaks on EDAX spectrum. The same is observed for B and C on Microfiber and Nano fiber samples respectively. There is however fewer deposits on Nano fiber sample compared to flat and microfiber on PMMA.

G shows DPSC on biomineralized deposit on nanofibers P4VP. H shows DPSC on microfiber PMMA. I display few carbonaceous Ca-P deposits on flat P4VP. J and K show deposits templated along the microfiber and Nanofibers on P4VP respectively. L-N displays carbonaceous deposits on Flat, Microfiber and Nanofiber PMMA non-induces samples. O shows DPSC on P4VP Nanofiber without induction and P shows the same on PMMA Microfiber. Compared to PMMA, P4VP shows more biomineralized deposits. Q shows dermal fibroblasts on P4VP under induction with DEX, S shows the same without induction. R and T show no cell control on P4VP microfiber with and without induction respectively. All fibers on controls show biomineralized deposits templated along the fibers but with fewer quantity compared to DPSC cells.

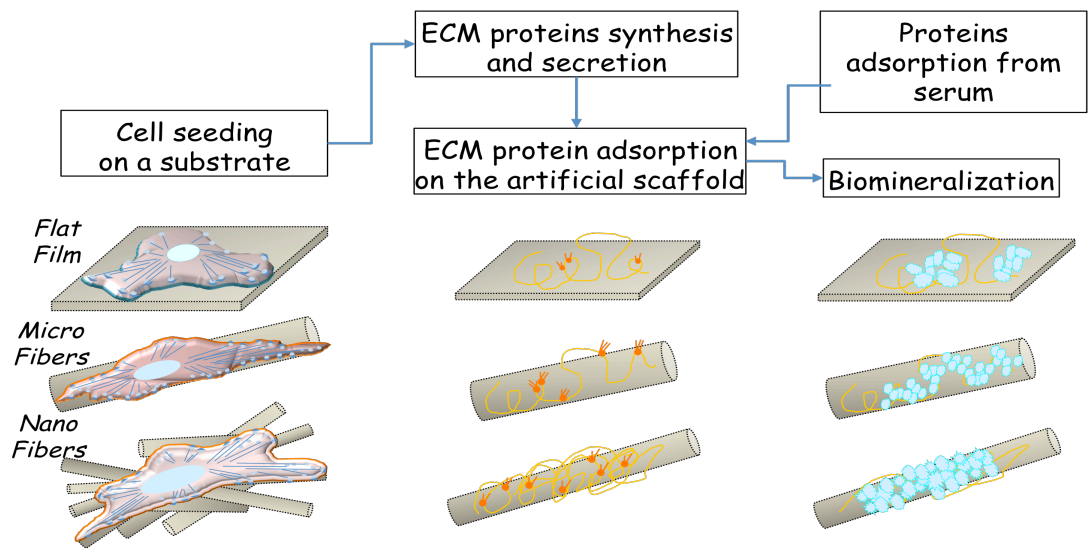


Figure 1.11 Protein mediated control of Cell Differentiation and Biomineralization

1

1

Chapter 2

Can Substrate Influence Lineage Choice

Introduction:

The controlled delivery of growth factors and cells within biomaterial carriers can enhance and accelerate target tissue formation specially bone [1]. For this purpose, BMP-2 which is FDA approved, has been used quite extensively for bone repair either exclusively or in combination with stem cells depending upon the desired outcome. Repair of large-scale bone defects require a robust response. This can involve using stem cells of embryonic origin, which have shown superior response, compared to adult mesenchymal stem cells [2]. Additionally, adequate and continuous delivery of soluble mediator (for e.g. BMP2) at the site of tissue is important since these proteins display shorter half life and are not cost-effective [3]. One recent method attempts to overcome these limitations by incorporating a transgene in the stem cells of choice, which is exogenously controlled by a drug [4, 5]. It is known that stem cells of embryonic origin exhibit higher potency and can potentially form many tissue types. Expression of BMP-2 in C3H10T1/2 cells (mesenchymal stem cells derived from mouse embryo) can induce differentiation of osteoblastic and chondroblastic cells [4, 6-8]. Since these stem cells are delivered on biomaterial we asked the following question: In the presence of BMP-2, can altering material mechanics or chemistry effect stem cell differentiation between osteogenic or chondrogenic lineage.

Although there is some data to suggest how stem cell behaves by varying substrate mechanics [9] but little is known how material factors such as surface chemistry can control stem cell behavior, initial protein and cell adhesion/morphology and ultimately differentiation. Recent study from our lab has identified some inherent limitations of using polyacrylamide gels to study mechanics by varying cross linkers [10]. This includes the residual surfactant

affecting cell behavior, collagen-I coating of these gels, since polyacrylamide does not favor direct cell growth ultimately impacting cell function and modulus at the gel surface. Our choice of biocompatible polymer to determine the effects of mechanics is Poly Butadiene (PB), a synthetic rubber, which resolves the limitations of polyacrylamide gels. PB at ~4MPa has shown to spontaneously cause differentiation of dental pulp stem cells (obviating the need for dexamethasone) [10].

In order to probe the effects of chemistry our polymer of choice is PSS₂₈. Partially sulfonated polystyrene is highly charged surface that can be induced to self assemble a fibrillar network of ECM proteins, particularly fibronectin [11, 12]. This is in contrast to conventional tissue culture polystyrene, which does not favor Fibrillogenesis. Rather the proteins stay globular. The increased sulfonation approx. 28% accounts for the surface charge and resulting fibrillogenesis that closely mimics the in-vivo environment. These studies utilized committed stem cells to probe effects of sulfonated polystyrene on cell behavior; therefore it is unknown how uncommitted mesenchymal stem cells of embryonic origin will respond to these substrates. Due to ethical considerations with use of human embryonic cells we choose C3H10T1/2 as mesenchymal cells of choice.

Additionally, we used tet-regulated gene expression of rhBMP-2 in C3H10T1/2 cells (C9 clone) to determine the effect of mechanics and chemistry in determining lineage choice, rhBMP-2 expression was controlled using the tet-off system in which binding of tetracycline to the transactivator inhibits transgene expression.

Material and Methods:

Sample Preparation:

To prepare various thicknesses of PB spun-cast films, monodisperse polybutadiene (Mw= 205,800, Mw/Mn = 1.49; Scientific Polymer Products, Inc.) were dissolved in Toluene (certified A.C.S.; ACROS) at different concentrations (w/v). The polished silicon wafers (Wafer World Corporation, West Palm Beach,

FL) used in this study were etched in hydrofluoric acid to make the surfaces hydrophobic. The PB solutions of 3 and 20 mg/mL were then spun-cast at 2,500 rpm onto HF-etched wafers to produce of PB films with thicknesses of 200 and 2000 Å as measured by ellipsometry. PB films were then annealed in the ultra-high vacuum oven at 10^{-8} torr at 150°C for 24 h to remove the residual solvent and further sterilize PB films for DPSC culture.

PSS₂₈ (Mw=200,000) was prepared by dissolving 1g of PS in 30 mL of dichloroethane in a 100-mL three-necked round-bottom flask. Acetic anhydride with concentrated sulfuric acid (molar ratio of 1.6:1) was added at room temperature. The reaction was allowed to proceed at 50°C for select times to obtain the required levels of sulfonation and then terminated by the addition of methanol. Solvent, byproducts methyl acetate, acetic acid and unreacted acid, and methanol were removed by steam tripping for 2 h. The SPS was dried in air for 24 h. Before spin coating, SPS was dissolved in dimethylformamide and PS in toluene. These solutions were then spun cast onto the silicon wafers, forming a monolayer.

Cell Culture and Induction:

The BMP-2 inducible expression cell line (C9 cell) was originated from C3H10T1/2 murine MSCs cell line after transfection with the human BMP-2 gene under control of the inducible Tet-off system [5]. The C9 cells and the parent strain C3H10T1/2 used as controls were cultured in basic medium: Dulbecco's Modified Eagle's Medium (DMEM) (Fisher, Pittsburg, PA) supplemented with 10% fetal bovine serum (Fisher), 2 mM L-glutamine, 100 U ml⁻¹ penicillin, 100 µg ml⁻¹ streptomycin (Invitrogen, Carlsbad, CA), and 1 µg/ml Dox (Sigma-Aldrich, St Louis, MO) to repress BMP-2 secretion (C9 cells only). For induction, C9 cells were cultured in differentiation medium: basic medium supplemented with 10 mM beta-glycerophosphate, 0.05 mM ascorbic acid-2-phosphate (Sigma-Aldrich) and with or without Dox added. Medium was changed every alternate day.

Shear modulation force microscopy (SMFM)

The moduli of DPSCs cultured on these films were measured by atomic force microscopy (AFM, Dimension 3000; Digital Instruments, Santa Barbara, CA) on shear modulation force microscopy (SMFM) mode. The experimental setup of the SMFM method is described in earlier articles. Briefly, the AFM tip, applied to indent the surface, was laterally modulated and the mechanical response was fed into a lock-in amplifier and recorded. During the measurement, a normal indenting force of 25nN was exerted by the cantilever to maintain tip-surface contact, while a sinusoidal drive signal was applied to the piezo controlling the cantilever to induce a small oscillatory motion. The lateral deflection (response) amplitude of the cantilever was measured against the drive amplitude, both in mV, the response amplitude, therefore, being proportional to drive amplitude. (Figure 3.1)

Laser scanning confocal microscopy (LSCM)

Immunocytochemistry was used to assess the state of the actin filaments, expression of osteocalcin and nuclear location. For that the DPSCs were washed with PBS, fixed with 3.7% formaldehyde solution for 15 minutes, permeabilized with 0.4% Triton X-100 in PBS and consequently incubated with 1:200 dilution of Alexa Fluor 488 Phalloidin solution (Invitrogen, Carlsbad, CA) for actin fiber detection. The nuclei were visualized when needed by propidium iodide (Sigma Chemical Co., St. Louis, CA). Samples were analyzed and images captured using Leica TCS SP2 LSCM (Leica micro-system Inc., Bannockburn, IL).

Scanning electron microscopy and energy dispersive X-ray (SEM/EDAX)

Surface morphologies of PB films were characterized using scanning electron microscopy (SEM, LEO1550, LEO, German) at 20 kV acceleration voltage and 10 mm working distance. Samples were prepared by gently washing with DI water to remove soluble salts from media and air-drying for 1 day. Samples were sputter-coated with gold for 15s and loaded on aluminum stubs for SEM imaging.

The elemental compositions of deposits on PB films were determined by using Energy dispersive X-ray spectroscopy in conjunction with SEM.

Real Time-Polymerase Chain Reaction

On day 14 after cell seeding the cells were trypsinized and resuspended as cell pellet. The cell pellet was lysed and stored at -80°C for a maximum period of one month. The total RNA was extracted from C9 and C3H10T1/2 on PB and SPS using Qiagen RNEasy kit (RNeasy kit, Qiagen, Valencia, CA). $1\mu\text{g}$ of total RNA was reverse-transcribed with 200 units/reaction Superscript II Reverse Transcriptase (Invitrogen) into cDNA using 200ng/reaction of random primers (Invitrogen). The obtained cDNA was used as a template in PCR. Specific markers for osteocalcin (OC), bone sialoprotein (BSP), alkaline phosphatase (ALP) and Osterix (OSX) monitored the osteogenic differentiation of cells. The chondrogenic markers were. The sequences of the specific primer sets are listed in Table 3.1 18SrRNA were used as a housekeeping gene to normalize mRNA expression. Due to its abundant expression the cDNA was diluted 100 times before use in the PCR. Real-time PCR was performed using SYBR Green PCR kit (Qiagen, Valencia, CA) and controlled in a DNA engine MJ Opticon 2 thermal Cycler with continuous fluorescence detection (MJ Research Incorporation, Union, NJ). DNA amplifications were performed under the following conditions: 95°C (15min), 94°C (30 s), 55°C (30 s), and 72°C (30 s) for 40 cycles, A melting curve program was performed immediately after the above cycling program in order to generate a first derivative dissociation curve for each sample and dilution series by using the instrument's software. Each sample was assessed in triplicate.

RESULTS

BMP-2 is upregulated in absence of Doxycycline

mRNA expression of BMP-2 for C9 cells was determined at Day 0 (out of culture flask), and for C9 and C3H10T1/2 at day 14 across all PB and PSS₂₈ samples.

(Fig 2.1) BMP-2 is upregulated in the absence of doxycycline on C9 cells across all surfaces while no expression was observed in the presence of Doxycycline and control cells. This ensures workability of our model system in order to determine the differentiation pathway of choice undertaken by C9 cells.

Cell Stiffness is influenced by surface mechanics and chemistry

On PB, cell modulus is dependant on BMP2 as it is highest on day 1 and falls to minimum on day 5 (Fig 2.2 A) Additionally in the presence of BMP-2 the moduli of the cells track with the modulus of the substrate on Day 1. The moduli of the control cells remains constant despite the 400% increase in substrate stiffness (1MPa for thick PB compared 4MPa for thin PB film). On PSS₂₈, modulus of all cells is high at Day 1 with a sharp drop by day 3 (Fig 2.2 B). Fibrillogenesis of cell ECM proteins occur spontaneously on PSS₂₈ (Fig 2.3.I A-J for C9 cells and Fig 2.3.II A-H for control cells). The change in modulus of these fibers indicates change in protein nature and conformation of the secreted ECM protein at early times (Fig 2.3.III-IV). This change in cell stiffness correlates with moduli of ECM fibers regardless of BMP-2. In the presence of BMP-2 on all surfaces C9 exhibits a smaller cell aspect ratio (Fig 2.4)

Gene Expression (RTPCR)

mRNA expression of a series of chondrogenic and osteogenic markers was measured on day 14. (fig 2.5 A-H) Choosing day 14 for gene expression provides window into the regulation of transcription factors, matrix and transitional markers involved. In the absence of chondroinductive and osteoinductive factors substrate determined lineage choice in the presence of BMP-2. PSS₂₈ enhanced BSP (substrate controlled) expression along with increased expression OSX, ALP, OCN and COL-X (which is under BMP-2 control regardless of substrate type and mechanics). PB predominantly expresses chondrogenic markers ACAN and SOX-9 (under substrate control) except Collagen IIA. On day 14 early osteogenic markers (osx & alp) are greater on thick PB whereas late marker ocn is greater on thin PB. This may suggest that mechanics may influence the

progression of differentiation of C9 cells. Additionally there is some effect direct effect of doxycycline as a function of mechanics in the absence of BMP-2 as control cells show mild upregulation of Osteocalcin progressing from thick film PB to thin film PB and eventually PSS₂₈.

Biom mineralization

SEM-EDAX at day 14 was used to analyze the presence of mineralized deposits and its distribution. On PB films, presence and absence of BMP-2 on PB (Fig.2.6 A-D) had remote effect as no biom mineralized deposits were found for C9 cells as well as controls. EDAX spectra showed mostly carbonaceous deposit. Only biom mineralized fibers and proteins are observed with SEM-EDAX In the absence of BMP-2 biom mineralization is observed only on a few ECM fibers. BMP-2 promotes biom mineralization in both the fibrillar and flat regions of the adsorbed ECM, forming a 1.4-micron thick biom mineralized film on PSS₂₈ (fig 2.7). The EDAX analyses identified Ca and P peaks indicating the mineralized deposits are hydroxyapatite crystals. Control cells show few biom mineralized deposits on PSS₂₈ with distribution similar to +DOX (BMP2 non induced C9 cells) data not shown.

Discussion:

In order to probe the influence of mechanical cues, PB films of two thicknesses were probed; 20nm (thin film) and 200nm (thick film), where the modulus of the thick film is bulk like, but surface interactions increase the modulus of the thinner film by a factor of 4. Hence the influence of mechanics can be directly compared in this system, in the absence of any chemical changes. The role of chemistry was probed by comparing the response of cells plated on sulfonated PS that is styenic.. The glass transition of PB, is below ambient, T_g=-40C, while that of PSS₂₈ =110C, is well above. Hence PB is a soft rubbery material, with a Yong's Modulus of 1.4 MPa while that of the harder, glassy PSS₂₈ is approx. 3GPa.

Osteogenic and chondrogenic markers were studied at day 14. This day was

chosen, as most matrix markers identifying lineage can be determined at this point. Additionally in spite of doxycycline control, BMP-2 secretion undergoes significant decrease, possibly due to the decrease in cell metabolism with time in culture [13].

Effect of Substrate Stiffness and BMP-2 on lineage specification

The effect of substrate mechanics on PB was not conclusive in our study apart from cell modulus, which showed BMP-2 dependant response. Gene expression data showed upregulation of chondrogenic markers (SOX-9 and ACAN) in C9 cells under BMP-2, modulated by PB surfaces indicating lineage towards chondrogenic pathway. This effect on PB rubber as a whole (no regard for mechanics) may account for the narrow range of substrate stiffness that correlates with neo-cartilage and chondrogenic tissue [14]. TGF- β has previously been used to induce stem cell differentiation into either smooth muscle cell lineage or chondrogenic lineage. A recent study found soft matrix in presence of TGF- β drives mesenchymal stem cells into chondrogenic cells whereas hard matrix into smooth muscle cells. The mechanical cue acts as an important determinant and co-factor for cell differentiation induced by soluble biochemical factors. Stem cells need to integrate micro environmental cues from both soluble biochemical factors and ECM to regulate differentiation [15]. In our study, the observed lack of biomineralization and upregulation of chondrogenic markers also provides insight into the different response of adult stem cells versus embryonic and/or human versus mouse cells. This is in light of the fact that thin film PB has shown to directly cause differentiation of dental pulp stem cells into osteoblasts or odontoblasts depending upon the presence or absence of dexamethasone [10].

The mild increase in modulus of C9 cells (compared to parent controls) cultured in presence of DOX (more on thin film PB than thick film) suggests minor BMP-2 leakiness in terms of transgene repression by DOX. This may occur due to 24-hour half-life of doxycycline compared to 48-hour standard culture media feeding schedule, therefore it might be useful to have transgene under Tet-On

control system (Clontech) where Doxycycline acts to up regulate expression rather than act as a repressor as in the Tet-Off system (Clontech).

Effect of Substrate Chemistry and BMP-2 on lineage specification:

Results from gene expression show substrate chemistry with increased sulfonation and resulting fibrillogenesis enhances differentiation of C9 cells in the presence of bmp-2 towards osteogenic pathway. All osteogenic markers were upregulated with BSP modulated by PSS₂₈, whereas the rest were under direct BMP-2 control. It is well described all implantable biomaterials are immediately coated with proteins from serum and subsequently ECM proteins produced by cells. Hence, it is the adsorbed proteins, rather than the surface itself, to which cells initially respond. Therefore it is these extracellular adhesion proteins (fibronectin and vitronectin in particular) that play a critical role in cell adhesion, morphology, and migration [16]. The pattern in which adhesion proteins and other bioactive molecules adsorb thus elicits cellular reactions specific to the underlying physicochemical properties of the material. Accordingly, *in vitro* studies generally demonstrate favorable cell responses to charged, hydrophilic surfaces, corresponding to superior adsorption and bioactivity of adhesion proteins [11, 12]. Our study highlights the importance of adsorbed proteins, which mediates stem cell responses to biomaterials, in the context of bone tissue engineering by osteoblast.

In contrast to PB all cells (C9 and controls) showed increased cell moduli on PSS₂₈ that correlates with eventual biomineralization observed on all these surfaces at day 14 on SEM. BMP-2 induction caused thicker and generalized distribution of CaP deposits whereas the C9 cells treated with DOX and controls showed focal areas of biomineralization. These results are consistent with those of Meng et al. [12] who compared the moduli of mineralizing and nonmineralizing MC3T3-E1 cells and found a similar increase only in the mineralizing cells. It is important to highlight that a thick film of CaP of ~1.4 microns at day 14 is quite remarkable considering most osteogenic and or biomineralization assays show

this to occur by day 28. (Fig 2.8) Perhaps few studies have looked into the effects embryonic mesenchymal stem cells and polymers that enable fibrillogenesis that most closely matches the in-vivo environment.

This robust response may be helpful in applications where enhanced osseointegration is required such dental and maxillofacial implants, plates and screws for bone fractures. However more studies are required to identify mechanical properties of PSS₂₈ for internal use as well as safety.

Conclusions:

- The impact of BMP-2 is modulated by surface chemistry
- PSS₂₈ promotes the expression of osteogenic markers by day 14
- PB promotes the expression of osteogenic and chondrogenic markers by day 14
- Surface mechanics may influence the progression of differentiation
- On day 14 early osteogenic markers (osx & alp) are greater on thick PB whereas late marker ocn is greater on thin PB
- Surface chemistry regulates biomineralization
- Growth on PSS₂₈ but not PB promotes biomineralization
- BMP-2 enhances biomineralization on PSS₂₈
- Surface chemistry and mechanics modify the impact of DOX on ocn expression

FIGURES AND TABLES

Primers	Forward	Reverse
18SrRNA	GTAACCCGTTGAACCCATT	CCATCCAATCGGTAGTAGCG
RUNX2	GAGCTCCGAAATGCCTCCGCT	GCTTCTGTCTGTGCCTTCTTGGT
SOX-9	AAGCTCTGGAGGCTGCTGAACGAG	GGTCGGCGGACCCTGAGATTG
Aggrecan	TCAACCGTTGCAGACCAGGAGCA	CAGGCTGGTTTGGACGCCACT
Col-X	CGCATCTCCAGCACCAGAATC	GGTGCCTCGAGGTCCGGTTG
Col2A	TGCCGCATCTGTGTGTGTGACAC	CCTTTCTGCCCTTTGGCCCTAA
Osterix	CCTGACTCCTTGGGACCCGGTC	CTGGGTAGGCGTCCCCCATGG
Osteocalcin	CTCACAGATGCCAAGCCCAGCG	TGCGTTTGTAGGCGGTCTTCAAG
ALP	TCCTGGGAGATGGTATGGGCGTC	GTTGCATCGCGTGCGCTCTG
BSP	TTTCCAGTCCAGGGAGGCAGTGA	TGGGCAGTTGGAGTGCCGCTAA
hBMP-2	GACCACCGGTTGGAGAGGGCA	GGTCACGGGGAATTTGAGTTGG

Table 2.1 Primer sequences for RTPCR mRNA analysis

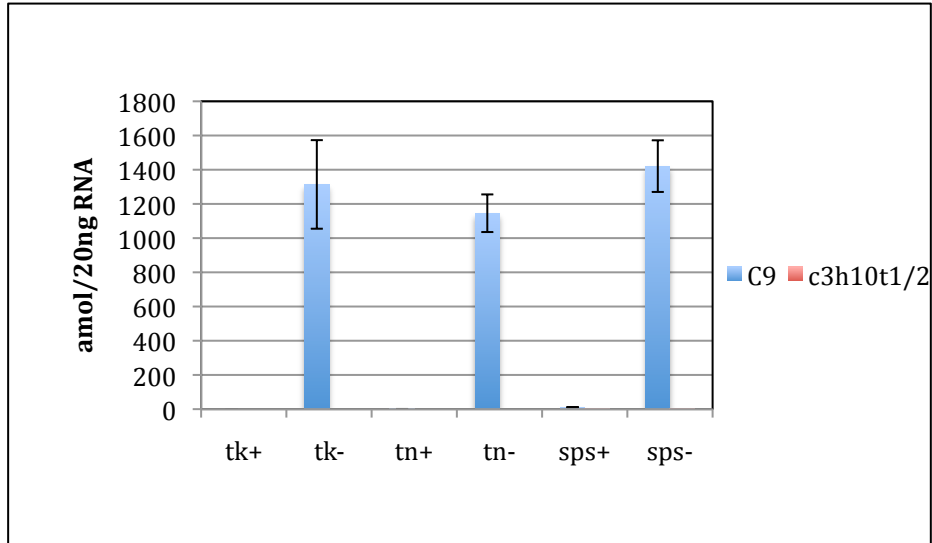
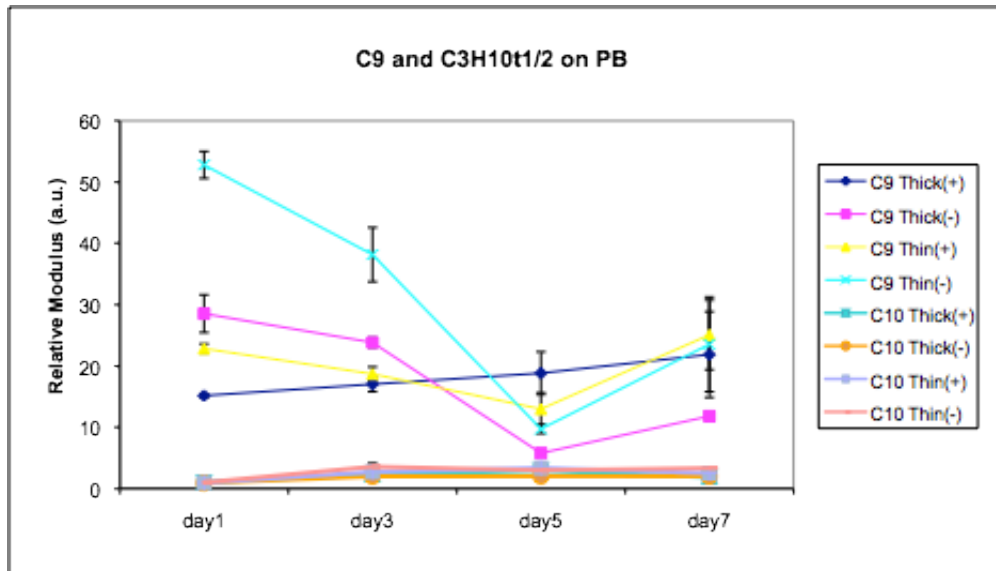
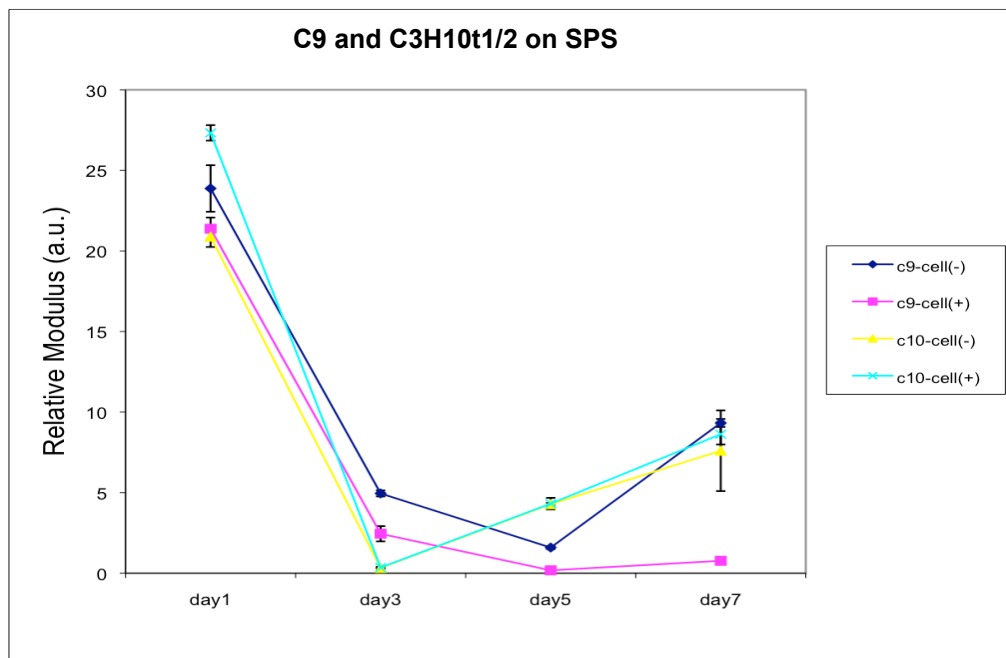
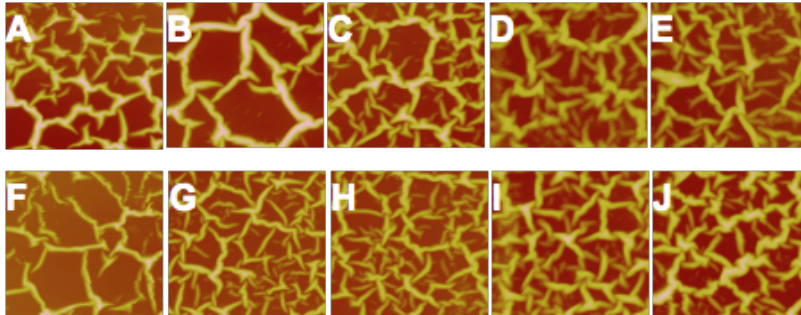


Figure 2.1 mRNA expression of h-BMP2 gene normalized to 18SrRNA
mRNA expression of human BMP-2 on C9 and parent strain (C3H10T1/2) by QPCR analysis on Day 7.

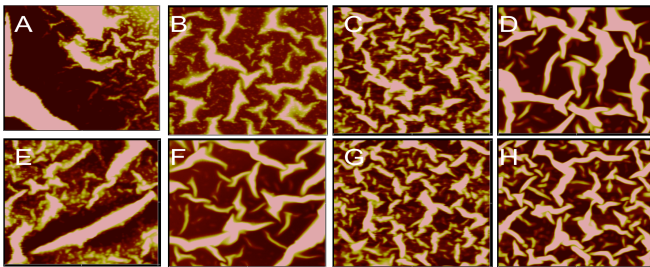
A**B****Figure 2.2 Cell Moduli on PB and SPS**

Atomic force microscopy and shear modulation force microscopy was used to measure the moduli (hardness) of cells for 1 week after cell plating on PB thin and thick film (A) and SPS (B). C9 have been transfected with rhBMP-2 gene regulated by Doxycycline. C10 is the parental strain C3H10T1/2 and used as controls.

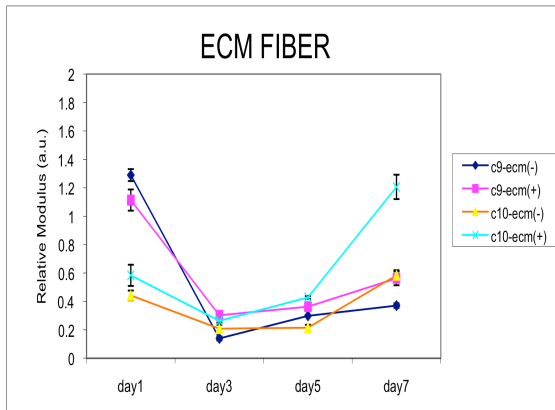
I



II



III



IV

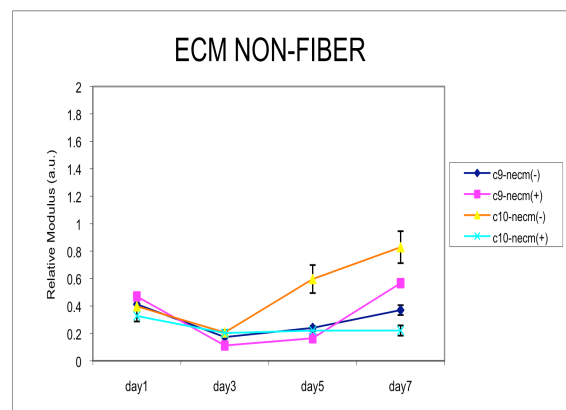


Figure 2.3 Modulus of ECM on PSS₂₈

Fibers formed on PSS₂₈ are visualized and modulus is measured by AFM/SMFM.

3.3.I A-E: C9 induced by BMP-2 i.e. -DOX (Day 2,4,6,8 and 10);

3.3.I F-J: C9 non-induced i.e. +DOX (Day 2,4,6,8 and 10).

3.3.II A-D C3H10T1/2 -DOX (Day 2,4,6,8)

3.3.II E-H C3H10T1/2 +DOX (Day 2,4,6,8)

3.3.III Modulus of Fibers ECM formed on PSS₂₈

3.3 IV Modulus of non-fiber area formed on PSS₂₈

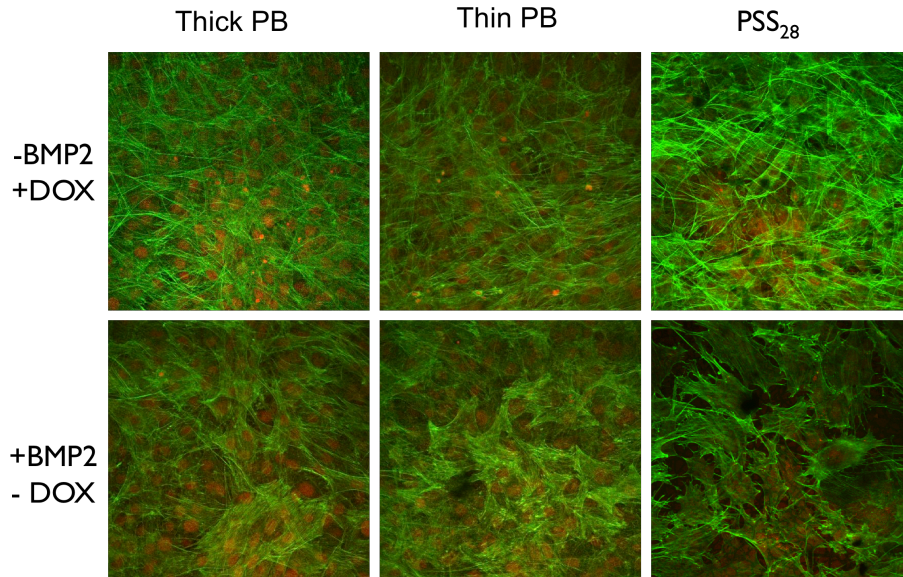


Figure 2.4 Cell Morphology is influenced by BMP-2

Confocal laser scanning microscopy images of C9 cells on Day 7 stained for actin (green) and nuclei (red) on thick and thin PB and SPS in the presence and absence of doxycycline (DOX)

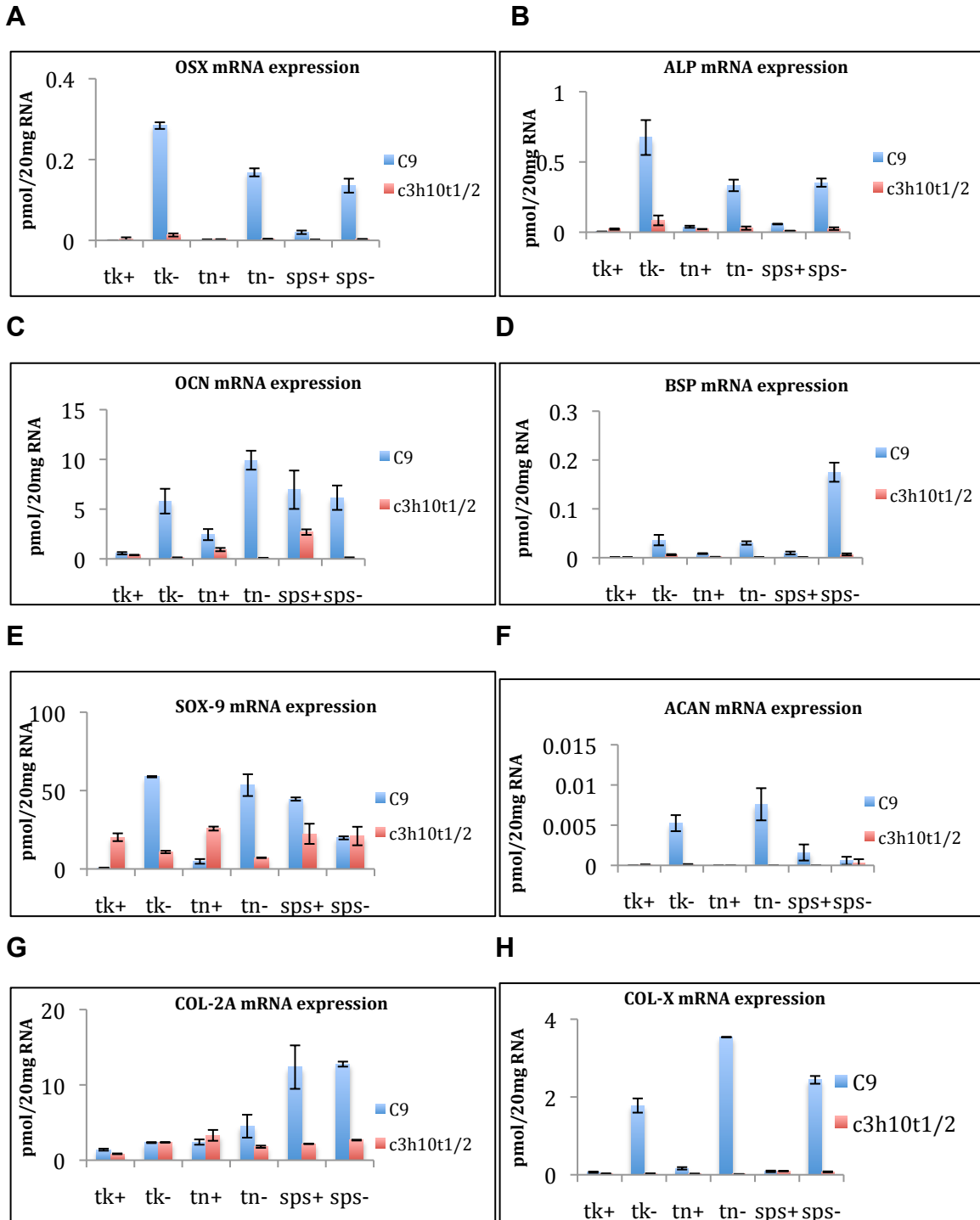


Figure 2.5 mRNA expression of Osteogenic and Chondrogenic markers
 mRNA expression at day 14. tk+=thick PB with DOX, tk-= thick PB without DOX, tn+= thin PB with DOX, tn-=thin PB without DOX, sps+= PSS₂₈ with DOX & sps- = PSS₂₈ without DOX. Fig 3.5 A-D shows osteogenic and E-H shows chondrogenic markers shown in absolute amount and normalized to internal gene 18SRNA.

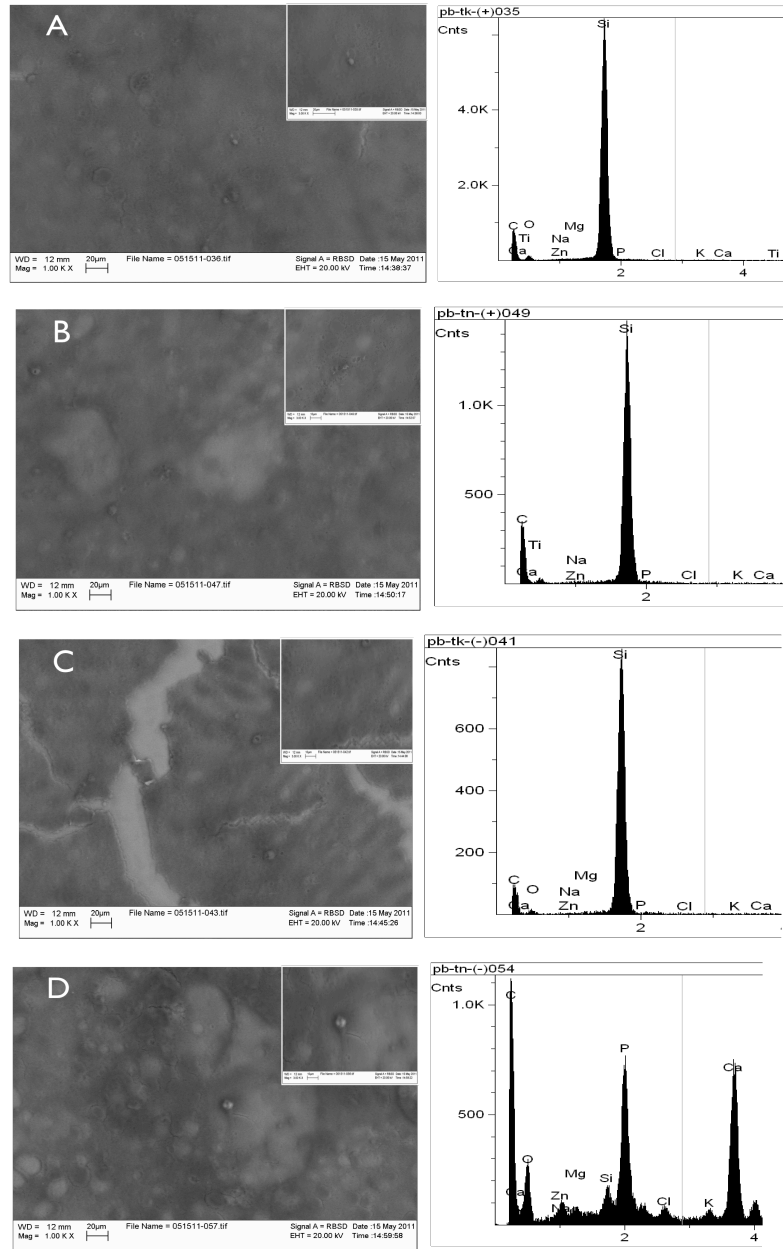


Figure 2.6 Analysis of biom mineralized deposits on PB (SEM-EDAX)
 C9 cells on A= thick film +DOX, B= thin film + DOX, C= thick film –DOX, D=thin film –DOX showing SEM images and EDAX spectrum.

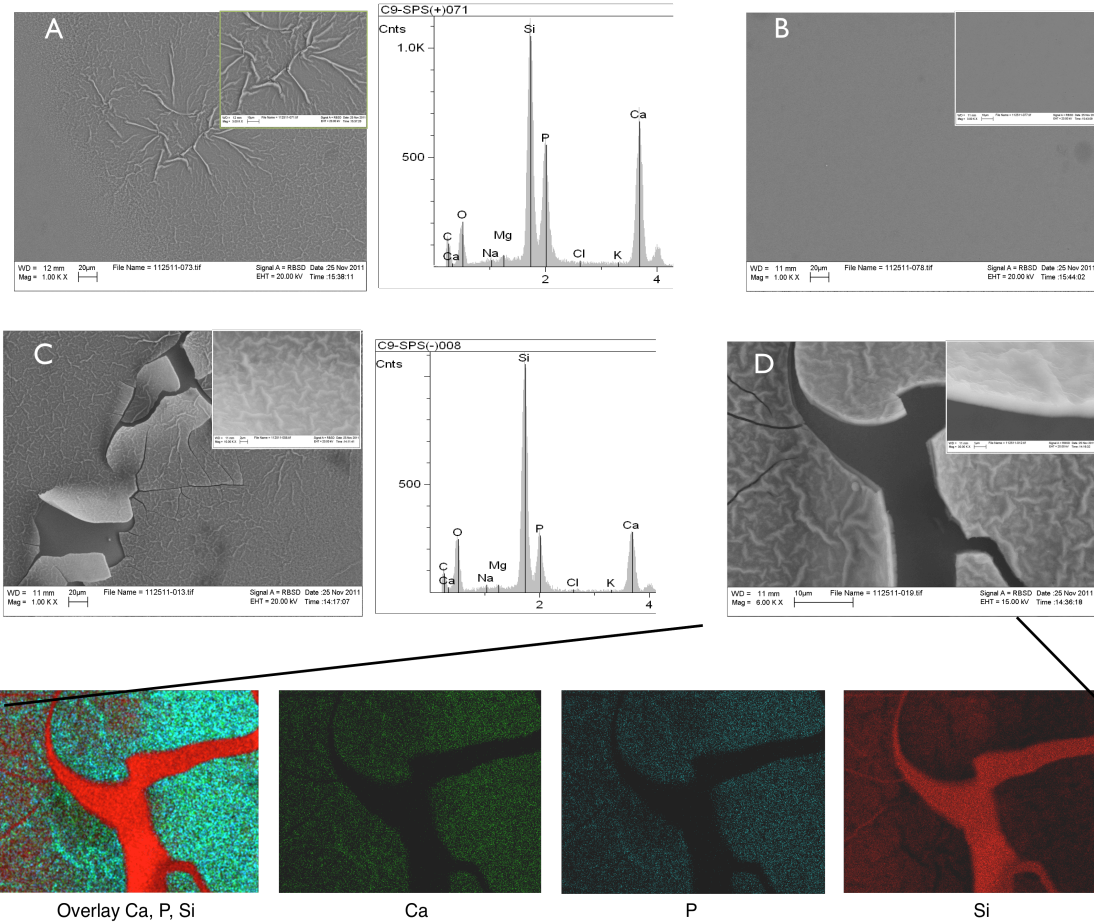


Figure 2.7 Analysis of Biom mineralized deposits on PSS28 (SEM-EDAX)

SEM image of ECM on PSS₂₈ secreted by cell culture treated with doxycycline (no BMP2 induction) (A) biom mineralized area (B) non biom mineralized area. In the absence of DOX C-D show generalized thick distribution of Ca-P film with biom mineralized fibers. EDXS mapping of calcium, phosphate and background silica of image (D) shows Ca and P deposits templated onto the fibers and in between.

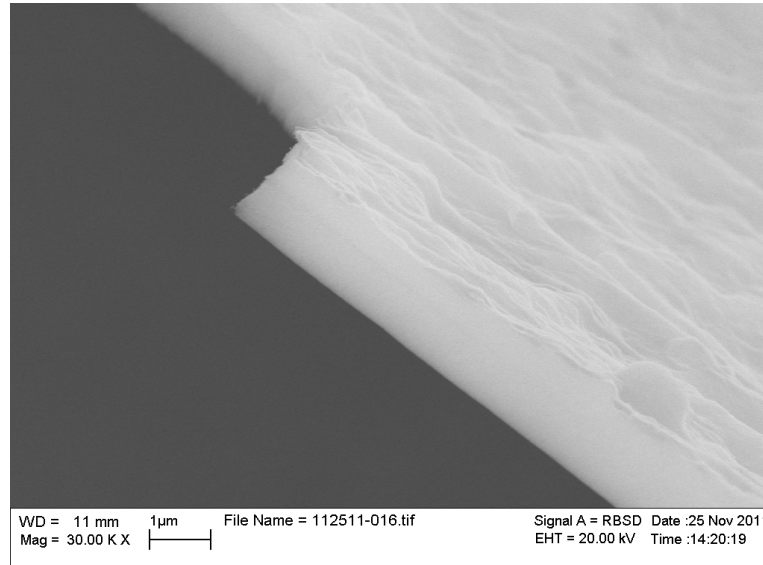


Figure 2.8 Thickness of Biomaterialized Film

SEM image of biomaterialized film on PSS₂₈ when C9 cells are induced by BMP-2 in the absence of DOX. The film thickness at the edge averages 1.319 μm compared to controls that measures 0.97 μm.

References:

Literature Review

1. Curran, J.M., R. Chen, and J.A. Hunt, *The guidance of human mesenchymal stem cell differentiation in vitro by controlled modifications to the cell substrate*. Biomaterials, 2006. **27**(27): p. 4783-93.
2. Khademhosseini, A., et al., *Microscale technologies for tissue engineering and biology*. Proc Natl Acad Sci U S A, 2006. **103**(8): p. 2480-7.
3. Park, T.H. and M.L. Shuler, *Integration of cell culture and microfabrication technology*. Biotechnol Prog, 2003. **19**(2): p. 243-53.
4. Bettinger, C.J., R. Langer, and J.T. Borenstein, *Engineering substrate topography at the micro- and nanoscale to control cell function*. Angew Chem Int Ed Engl, 2009. **48**(30): p. 5406-15.
5. Okita, K., T. Ichisaka, and S. Yamanaka, *Generation of germline-competent induced pluripotent stem cells*. Nature, 2007. **448**(7151): p. 313-7.
6. Friedenstein, A.J., R.K. Chailakhyan, and U.V. Gerasimov, *Bone marrow osteogenic stem cells: in vitro cultivation and transplantation in diffusion chambers*. Cell Tissue Kinet, 1987. **20**(3): p. 263-72.
7. Anderson, D.J., F.H. Gage, and I.L. Weissman, *Can stem cells cross lineage boundaries?* Nat Med, 2001. **7**(4): p. 393-5.
8. Woodbury, D., et al., *Adult rat and human bone marrow stromal cells differentiate into neurons*. J Neurosci Res, 2000. **61**(4): p. 364-70.
9. Ferrari, G., et al., *Muscle regeneration by bone marrow-derived myogenic progenitors*. Science, 1998. **279**(5356): p. 1528-30.
10. Huang, G.T., S. Gronthos, and S. Shi, *Mesenchymal stem cells derived from dental tissues vs. those from other sources: their biology and role in regenerative medicine*. J Dent Res, 2009. **88**(9): p. 792-806.
11. Yamamura, T., *Differentiation of pulpal cells and inductive influences of various matrices with reference to pulpal wound healing*. J Dent Res, 1985. **64 Spec No**: p. 530-40.
12. Baume, L.J., *The biology of pulp and dentine. A historic, terminologic-taxonomic, histologic-biochemical, embryonic and clinical survey*. Monogr Oral Sci, 1980. **8**: p. 1-220.
13. Nakashima, M., *Bone morphogenetic proteins in dentin regeneration for potential use in endodontic therapy*. Cytokine Growth Factor Rev, 2005. **16**(3): p. 369-76.
14. Gronthos, S., et al., *Postnatal human dental pulp stem cells (DPSCs) in vitro and in vivo*. Proc Natl Acad Sci U S A, 2000. **97**(25): p. 13625-30.
15. Gronthos, S., et al., *Stem cell properties of human dental pulp stem cells*. J Dent Res, 2002. **81**(8): p. 531-5.
16. Miura, M., et al., *SHED: stem cells from human exfoliated deciduous teeth*. Proc Natl Acad Sci U S A, 2003. **100**(10): p. 5807-12.

17. Shi, S., et al., *The efficacy of mesenchymal stem cells to regenerate and repair dental structures*. *Orthod Craniofac Res*, 2005. **8**(3): p. 191-9.
18. Shi, S., P.G. Robey, and S. Gronthos, *Comparison of human dental pulp and bone marrow stromal stem cells by cDNA microarray analysis*. *Bone*, 2001. **29**(6): p. 532-9.
19. Yamada, Y., et al., *Cluster analysis and gene expression profiles: a cDNA microarray system-based comparison between human dental pulp stem cells (hDPSCs) and human mesenchymal stem cells (hMSCs) for tissue engineering cell therapy*. *Biomaterials*, 2006. **27**(20): p. 3766-81.
20. Zhang, W., et al., *Multilineage differentiation potential of stem cells derived from human dental pulp after cryopreservation*. *Tissue Eng*, 2006. **12**(10): p. 2813-23.
21. Iohara, K., et al., *Side population cells isolated from porcine dental pulp tissue with self-renewal and multipotency for dentinogenesis, chondrogenesis, adipogenesis, and neurogenesis*. *Stem Cells*, 2006. **24**(11): p. 2493-503.
22. Yang, X., et al., *The odontogenic potential of STRO-1 sorted rat dental pulp stem cells in vitro*. *J Tissue Eng Regen Med*, 2007. **1**(1): p. 66-73.
23. Simmons, P.J. and B. Torok-Storb, *Identification of stromal cell precursors in human bone marrow by a novel monoclonal antibody, STRO-1*. *Blood*, 1991. **78**(1): p. 55-62.
24. Gronthos, S., et al., *The STRO-1+ fraction of adult human bone marrow contains the osteogenic precursors*. *Blood*, 1994. **84**(12): p. 4164-73.
25. Dennis, J.E., et al., *The STRO-1+ marrow cell population is multipotential*. *Cells Tissues Organs*, 2002. **170**(2-3): p. 73-82.
26. Sheyn, D., et al., *Genetically modified cells in regenerative medicine and tissue engineering*. *Adv Drug Deliv Rev*, 2010. **62**(7-8): p. 683-98.
27. Peng, H., et al., *Development of a self-inactivating tet-on retroviral vector expressing bone morphogenetic protein 4 to achieve regulated bone formation*. *Mol Ther*, 2004. **9**(6): p. 885-94.
28. Moutsatsos, I.K., et al., *Exogenously regulated stem cell-mediated gene therapy for bone regeneration*. *Mol Ther*, 2001. **3**(4): p. 449-61.
29. Simonis, P., T. Dufour, and H. Tenenbaum, *Long-term implant survival and success: a 10-16-year follow-up of non-submerged dental implants*. *Clin Oral Implants Res*, 2010. **21**(7): p. 772-7.
30. Apostol M, M.T., Yang NL, Pernodet N, Rafailovich MH, *Cell sheet patterning using photo-cleavable polymers*. *Polymer Journal*, 2011. **43**(August): p. 723-732.
31. Ozay, O., et al., *P(4-VP) based nanoparticles and composites with dual action as antimicrobial materials*. *Colloids Surf B Biointerfaces*, 2010. **79**(2): p. 460-6.
32. Li, M., et al., *Electrospun protein fibers as matrices for tissue engineering*. *Biomaterials*, 2005. **26**(30): p. 5999-6008.
33. Li, W.J., et al., *Fabrication and characterization of six electrospun poly(alpha-hydroxy ester)-based fibrous scaffolds for tissue engineering applications*. *Acta Biomater*, 2006. **2**(4): p. 377-85.
34. Sill, T.J. and H.A. von Recum, *Electrospinning: applications in drug delivery and tissue engineering*. *Biomaterials*, 2008. **29**(13): p. 1989-2006.

35. Cheng, S.L., et al., *Differentiation of human bone marrow osteogenic stromal cells in vitro: induction of the osteoblast phenotype by dexamethasone*. *Endocrinology*, 1994. **134**(1): p. 277-86.
36. Hamidouche, Z., et al., *Priming integrin alpha5 promotes human mesenchymal stromal cell osteoblast differentiation and osteogenesis*. *Proc Natl Acad Sci U S A*, 2009. **106**(44): p. 18587-91.
37. Lian, J.B., et al., *Regulatory controls for osteoblast growth and differentiation: role of Runx/Cbfa/AML factors*. *Crit Rev Eukaryot Gene Expr*, 2004. **14**(1-2): p. 1-41.
38. Franceschi, R.T. and G. Xiao, *Regulation of the osteoblast-specific transcription factor, Runx2: responsiveness to multiple signal transduction pathways*. *J Cell Biochem*, 2003. **88**(3): p. 446-54.
39. Hamidouche, Z., et al., *FHL2 mediates dexamethasone-induced mesenchymal cell differentiation into osteoblasts by activating Wnt/beta-catenin signaling-dependent Runx2 expression*. *FASEB J*, 2008. **22**(11): p. 3813-22.
40. Groeneveld, E.H. and E.H. Burger, *Bone morphogenetic proteins in human bone regeneration*. *Eur J Endocrinol*, 2000. **142**(1): p. 9-21.
41. Lane, J.M., *BMPs: why are they not in everyday use?* *J Bone Joint Surg Am*, 2001. **83-A Suppl 1**(Pt 2): p. S161-3.
42. Service, R.F., *Tissue engineers build new bone*. *Science*, 2000. **289**(5484): p. 1498-500.
43. Matsuda, T. and S. Nagahara, *mRNA expression induced by cell-substrate interaction. A two-dimensional tissue formation process*. *ASAIO J*, 1995. **41**(3): p. M398-403.
44. Deryugina, E.I. and M.A. Bourdon, *Tenascin mediates human glioma cell migration and modulates cell migration on fibronectin*. *J Cell Sci*, 1996. **109** (Pt 3): p. 643-52.
45. Engler, A.J., et al., *Matrix elasticity directs stem cell lineage specification*. *Cell*, 2006. **126**(4): p. 677-89.
46. Kim, T.J., et al., *Substrate rigidity regulates Ca²⁺ oscillation via RhoA pathway in stem cells*. *J Cell Physiol*, 2009. **218**(2): p. 285-93.
47. Pamula, E., et al., *Nanoscale organization of adsorbed collagen: influence of substrate hydrophobicity and adsorption time*. *J Colloid Interface Sci*, 2004. **271**(1): p. 80-91.
48. Bozec, L., G. van der Heijden, and M. Horton, *Collagen fibrils: nanoscale ropes*. *Biophys J*, 2007. **92**(1): p. 70-5.
49. Park, J., et al., *Nanosize and vitality: TiO₂ nanotube diameter directs cell fate*. *Nano Lett*, 2007. **7**(6): p. 1686-91.
50. Dalby, M.J., et al., *The control of human mesenchymal cell differentiation using nanoscale symmetry and disorder*. *Nat Mater*, 2007. **6**(12): p. 997-1003.
51. Ruiz, S.A. and C.S. Chen, *Emergence of patterned stem cell differentiation within multicellular structures*. *Stem Cells*, 2008. **26**(11): p. 2921-7.
52. Salasznyk, R.M., et al., *Focal adhesion kinase signaling pathways regulate the osteogenic differentiation of human mesenchymal stem cells*. *Exp Cell Res*, 2007. **313**(1): p. 22-37.

53. Posner AS, T.P., *The mineral phase of dentin*, in *Dentin and Dentinogenesis*, L. A, Editor 1984, CRC PRESS: Boca Raton, FLA.
54. Weiner, S.W., *THE MATERIAL BONE: Structure-Mechanical Function Relations*. Ann. ReV. Mater. Sci, 1998. **28**: p. 271-298.

Chapter One

1. Barry, F., et al., *Chondrogenic differentiation of mesenchymal stem cells from bone marrow: differentiation-dependent gene expression of matrix components*. Exp Cell Res, 2001. **268**(2): p. 189-200.
2. Chang, P.L., et al., *Comparison of fetal and adult marrow stromal cells in osteogenesis with and without glucocorticoids*. Connect Tissue Res, 2006. **47**(2): p. 67-76.
3. Weinstein, R.S., et al., *Inhibition of osteoblastogenesis and promotion of apoptosis of osteoblasts and osteocytes by glucocorticoids. Potential mechanisms of their deleterious effects on bone*. J Clin Invest, 1998. **102**(2): p. 274-82.
4. Engler, A.J., et al., *Matrix elasticity directs stem cell lineage specification*. Cell, 2006. **126**(4): p. 677-89.
5. Dalby, M.J., et al., *The control of human mesenchymal cell differentiation using nanoscale symmetry and disorder*. Nat Mater, 2007. **6**(12): p. 997-1003.
6. Apostol M, M.T., Yang NL, Pernodet N, Rafailovich MH *Cell sheet patterning using photo-cleavable polymers*. Polymer Journal, 2011. **43**(June): p. 723-732.
7. Pereira, L.O., et al., *Comparison of stem cell properties of cells isolated from normal and inflamed dental pulps*. Int Endod J, 2012.
8. Alvarez Perez, M.A., et al., *In vitro mineralization and bone osteogenesis in poly(epsilon-caprolactone)/gelatin nanofibers*. J Biomed Mater Res A, 2012.
9. Wilson, C.J., et al., *Mediation of biomaterial-cell interactions by adsorbed proteins: a review*. Tissue Eng, 2005. **11**(1-2): p. 1-18.
10. Ito, K., et al., *Osteogenic potential of effective bone engineering using dental pulp stem cells, bone marrow stem cells, and periosteal cells for osseointegration of dental implants*. Int J Oral Maxillofac Implants, 2011. **26**(5): p. 947-54.
11. Woo, K.M., V.J. Chen, and P.X. Ma, *Nano-fibrous scaffolding architecture selectively enhances protein adsorption contributing to cell attachment*. J Biomed Mater Res A, 2003. **67**(2): p. 531-7.
12. den Braber, E.T., et al., *Orientation of ECM protein deposition, fibroblast cytoskeleton, and attachment complex components on silicone microgrooved surfaces*. J Biomed Mater Res, 1998. **40**(2): p. 291-300.

Chapter Two

1. Vo, T.N., F.K. Kasper, and A.G. Mikos, *Strategies for controlled delivery of growth factors and cells for bone regeneration*. Adv Drug Deliv Rev, 2012.
2. Shimko, D.A., et al., *Comparison of in vitro mineralization by murine embryonic and adult stem cells cultured in an osteogenic medium*. Tissue Eng, 2004. **10**(9-10): p. 1386-98.
3. Sheyn, D., et al., *Genetically modified cells in regenerative medicine and tissue engineering*. Adv Drug Deliv Rev, 2010. **62**(7-8): p. 683-98.
4. Gazit, D., et al., *Engineered pluripotent mesenchymal cells integrate and differentiate in regenerating bone: a novel cell-mediated gene therapy*. J Gene Med, 1999. **1**(2): p. 121-33.
5. Moutsatsos, I.K., et al., *Exogenously regulated stem cell-mediated gene therapy for bone regeneration*. Mol Ther, 2001. **3**(4): p. 449-61.
6. Ahrens, M., et al., *Expression of human bone morphogenetic proteins-2 or -4 in murine mesenchymal progenitor C3H10T1/2 cells induces differentiation into distinct mesenchymal cell lineages*. DNA Cell Biol, 1993. **12**(10): p. 871-80.
7. Yamaguchi, A., et al., *Effects of BMP-2, BMP-4, and BMP-6 on osteoblastic differentiation of bone marrow-derived stromal cell lines, ST2 and MC3T3-G2/PA6*. Biochem Biophys Res Commun, 1996. **220**(2): p. 366-71.
8. Lou, J., et al., *Gene therapy: adenovirus-mediated human bone morphogenetic protein-2 gene transfer induces mesenchymal progenitor cell proliferation and differentiation in vitro and bone formation in vivo*. J Orthop Res, 1999. **17**(1): p. 43-50.
9. Engler, A.J., et al., *Matrix elasticity directs stem cell lineage specification*. Cell, 2006. **126**(4): p. 677-89.
10. C, C., *Osteogenic Dental pulp stem cells (DPSCs) differentiation is regulated by the mechanics of polybutadiene rubber films*, in *Material Sciences Department 2012*, Stony Brook University.
11. Pernodet, N., et al., *Fibronectin fibrillogenesis on sulfonated polystyrene surfaces*. J Biomed Mater Res A, 2003. **64**(4): p. 684-92.
12. Meng, Y., et al., *Biomaterialization of a self-assembled extracellular matrix for bone tissue engineering*. Tissue Eng Part A, 2009. **15**(2): p. 355-66.
13. Y, Z., *Regulation and patterning of cell differentiation and pluripotency*, in *Graduate School of Arts and Sciences 2011*, Columbia University. p. 1-175.
14. Schuh, E., et al., *Effect of matrix elasticity on the maintenance of the chondrogenic phenotype*. Tissue Eng Part A, 2010. **16**(4): p. 1281-90.
15. Park, J.S., et al., *The effect of matrix stiffness on the differentiation of mesenchymal stem cells in response to TGF-beta*. Biomaterials, 2011. **32**(16): p. 3921-30.
16. Wilson, C.J., et al., *Mediation of biomaterial-cell interactions by adsorbed proteins: a review*. Tissue Eng, 2005. **11**(1-2): p. 1-18.